TESTING PERIODICITY OF DEPOSITIONAL CYCLICITY, CISCO GROUP (VIRGILIAN AND WOLFCAMPIAN), TEXAS

WAN YANG[1] AND MICHELLE A. KOMINZ[2]
[1] *Department of Geology, Wichita State University, Wichita, Kansas 67260, U.S.A.*
e-mail: wyang@twsuvm.uc.twsu.edu
[2] *Department of Geology, Western Michigan University, Kalamazoo, Michigan 49008-5150, U.S.A.*

ABSTRACT: **Periodicities of 15 cyclic sections of the Cisco Group are tested through gamma and spectral analyses. The sections are composed of marine and nonmarine carbonate and siliciclastic rocks deposited on the Eastern Shelf, north-central Texas, in Late Pennsylvanian and Early Permian time. Gamma analysis generates facies-dependent thickness–time conversion factors (γ's) to construct γ-corrected time series, which are more realistic than the uncorrected series obtained by proportional conversion. Positive and stable γ's and improved resolution of the corrected spectra indicate successful γ tuning. On the Cisco spectra, a short-eccentricity peak (95–131 ky) is the most prominent and persistent; long-eccentricity (413 ky) and obliquity (34 and 43 ky) peaks are persistent, and precessional index peaks (17 and 21 ky) are less persistent. A persistent peak of period ~ 50–80 ky may be a combination tone between obliquity and precessional index cycles. Non-Milankovitch peaks are sporadic. The validity of gamma and spectral results is indicated by consistent γ-estimated ages among the Cisco sections and reasonable effective sedimentation rates calculated on the basis of Milankovitch spectral calibrations. The results, combined with geologic evidence, suggest that the Cisco cyclicity was controlled dominantly by Milankovitch climatic forcing.**

INTRODUCTION

Meter-scale depositional cycles are common in the geologic record (e.g., Gilbert 1895; Barrell 1917; Wanless and Shepard 1936; Fisher 1964; Grotzinger 1986; Goldhammer et al. 1994). High-frequency eustasy has been demonstrated as an important control on shallow marine and marginal marine cyclic sedimentation, and are commonly inferred to be related to Milankovitch climatic cycles (e.g., Fisher 1964; Wilson 1967; Heckel 1986; Goldhammer et al. 1990). The inference is drawn from Plio-Pleistocene analogs, which are closely related to Milankovitch cycles (Mesolella et al. 1969; Hays et al. 1976; Kominz and Pisias 1979; Cronin 1983; Imbrie et al. 1984; Chappell and Shackleton 1986; Berger 1988).

Average cycle period and cycle bundling similar to those of Milankovitch cycles have been used to suggest a Milankovitch origin for high-frequency eustasy and meter-scale cyclicity (e.g., Fischer 1964; Heckel 1986; Goldhammer et al. 1990). Spectra of cyclic sections that resemble the Milankovitch spectrum also provide strong support because Milankovitch climatic series have unique signatures in time and frequency (e.g., Olsen 1986; Hinnov and Goldhammer 1991).

However, a Milankovitch origin for depositional cyclicity remains debatable because of the assumptions in these tests, such as a constant sedimentation rate for different lithofacies, perfect chronostratigraphic time scales, equal duration for all cycles, and stratigraphic completeness. Commonly, tuning of time series and spectra is also required (e.g., Park and Herbert 1987; Kominz and Bond 1990; Kominz et al. 1991; Bond et al. 1991; Bond et al. 1993; Herbert 1992; Yang et al. 1995). Moreover, rigorous quantitative tests of multiple cyclic sections distributed regionally and formed in a period of extensive continental glaciation similar to the Pleistocene have not yet been reported.

This study tests whether Milankovitch signals are present in 15 Cisco sections. The Cisco cycles were formed by the interplay among high-frequency eustasy and many other autogenic and allogenic processes in Late Pennsylvanian and Early Permian time when continental glaciation was active (e.g., Lee 1938; Galloway 1971; Harrison 1973; Crowell 1978; Veevers and Powell 1987; Boardman and Heckel 1989; Brown et al. 1990; Yang 1995, 1996; Yang et al. 1998). The Cisco Group is an excellent record to test for a Milankovitch origin of depositional cyclicity and to evaluate the roles of various processes in modifying and destroying the Milankovitch signals, if present, during cyclic sedimentation.

GEOLOGY

Depositional Cyclicity of the Cisco Group

Nonmarine and marine siliciclastic and carbonate rocks of the Cisco Group were deposited on the Eastern Shelf of Midland Basin in the paleo–equatorial belt (Figs. 1, 2). The shelf dipped gently to the WNW and was surrounded by structural uplifts in the other directions (Fig. 1B; Wermund and Jenkins 1969; Brown et al. 1987). The shelf edge aggraded 400 m and prograded 200 km during the Cisco time (Fig. 1C; Brown et al. 1990).

The study area is ~ 300 km by 40 km in the outcrop belt, and ~ 100 km by 30 km in the subsurface (Fig. 3). 34 to 43 transgressive–regressive cycles are delineated on three composite outcrop sections, which are constructed from 88 measured sections along three traverses (Figs. 3, 4A, 5; Yang 1995). Transgressive deposits include delta-plain, marginal marine, shelf, and basin-slope siliciclastics, and shallow-marine carbonates. Regressive deposits include paleosols, fluvial, deltaic, and shelf siliciclastics, and subtidal to supratidal carbonates (Fig. 4A; Yang 1996). In the subsurface, 68 cycles are delineated in 71 wells on six cross sections (Figs. 3, 4B, 6; Yang et al. 1998). The component lithofacies are similar to those in the outcrop.

In addition to component lithofacies, Cisco cycles are characterized by thickness, magnitude, and stacking patterns (Yang 1996; Yang et al. 1998). Cycle magnitude is defined as the maximum facies shift in a cycle, indicating the extent of marine transgression (Fig. 4A). Three orders of cycles, termed minor, intermediate, and major, are identified. A major cycle contains one to several intermediate cycles, each of which contains one to several minor cycles (Fig. 7). In a major cycle, a minor cycle has the smallest magnitude and the major cycle has the largest magnitude. Therefore, a minor cycle has shorter duration than the intermediate cycle, which has shorter duration than the major cycle. Lateral correlation indicates that minor cycles represent transgressive–regressive events of short duration and variable areal extent, whereas major cycles represent events of long duration and shelf-wide extent (e.g., Fig. 6; Yang et al. 1998).

Cisco cyclicity varies along depositional strike and dip. In the outcrop, cycle continuity is poor because of the proximity to siliciclastic sources. Cycle abundance is high in the Brazos traverse, where frequent pulses of local fault-induced subsidence and clastic influx from northern source areas caused local transgressions and regressions. Cycles are more persistent in the Colorado traverse, where tectonic stability increases and variability of clastic influx decreases (Fig. 5; Yang 1995).

Subsurface cycles are well developed, and cycle continuity and abundance are high (Fig. 6; Yang et al. 1998). In the up-dip part, minor cycles are discontinuous and vary greatly in thickness, and many intermediate

JOURNAL OF SEDIMENTARY RESEARCH, VOL. 69, NO. 6, NOVEMBER, 1999, P. 1209–1231
 1073-130X/99/069-1210/$03.00

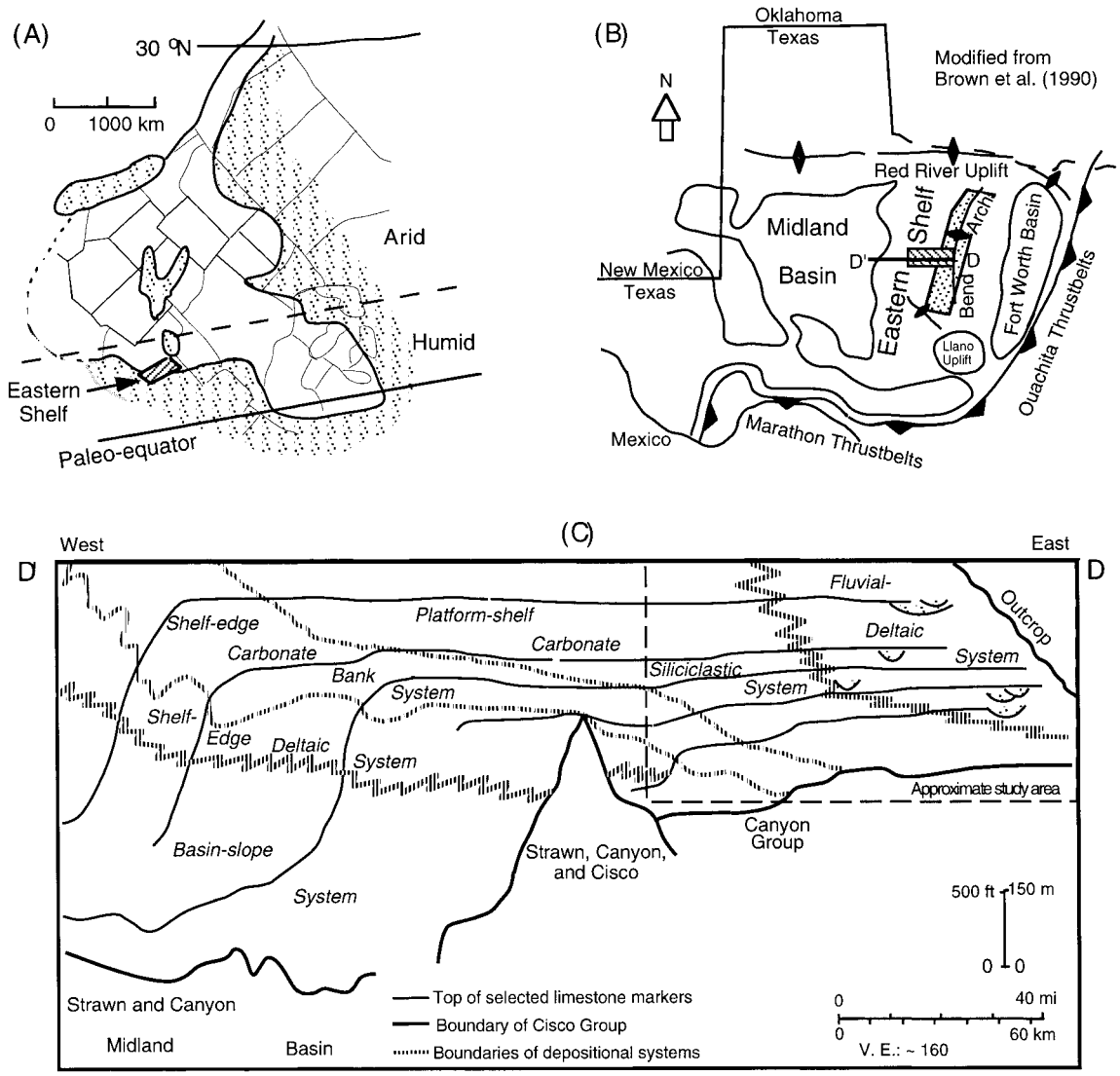

FIG. 1.—**A)** Approximate paleogeographic location of Eastern Shelf (hachured area) in the humid zone north of the paleo-equator in the western U.S. during Missourian and Virgilian time. Land areas (stippled) and continental margins during maximum marine onlap are schematic. Simplified from Witzke (1990). **B)** Regional tectonic elements surrounding the Eastern Shelf of Midland Basin, Texas. Outcrop (stippled) and subsurface (hachured) study areas are shown. **C)** Simplified dip cross section D–D′ of Brown et al. (1987) showing the stratigraphic architecture of Cisco Group and approximate cross-sectional area of this study.

cycles are fragmentary as a result of fluvial erosion and siliciclastic suppression of carbonate deposition, suggesting dominant autogenic influences. In the down-dip part, cycles are continuous and consistent in thickness, indicating diminishing autogenic influences (Fig. 6).

A variety of autogenic and allogenic processes are interpreted through correlation of cycle character and stacking patterns, and analysis of cycle symmetry (Yang 1995, 1996; Yang et al. 1998). Cycle absence and irregular variations of cycle character were controlled by local topography, local fault-induced subsidence, depositional locus switching, and differential compaction. In contrast, regional cycle continuity and systematic variations of cycle character were controlled by: (1) high-frequency eustasy controlling the extent and order of regional transgression and regression, (2) regional topography controlling sediment distribution, (3) timing, type, and amount of sediment supply controlling cycle thickness and component lithofacies, (4) climatic changes controlling sediment yield in the source areas, and (5) shelf subsidence controlling cycle preservation. In summary, high-frequency eustasy was a major control on cycle formation, although autogenic and allogenic signals are mixed in the Cisco record (Yang 1996; Yang et al. 1998). Here we present quantitative tests for the periodicity of depositional cyclicity and the origin of high-frequency eustasy.

Three composite outcrop sections and 12 wells are analyzed in our tests (Figs. 3, 5, 7). Eleven wells penetrate the entire Cisco Group except Well 24. Environmental interpretations are shown as facies curves on a grid with its vertical axis as thickness and its horizontal axis as environments (Figs. 4, 7). The environments are coded and facies curves are digitized to facilitate numerical data processing.

GAMMA ANALYSIS AND SPECTRAL ANALYSIS

The origin of Cisco cyclicity is tested by comparing the periods and relative magnitudes of Cisco spectral peaks with those of major late Paleozoic Milankovitch peaks predicted by Berger et al. (1992). The multiwindow prolate spectral analysis method of Thomson (1982) is used to

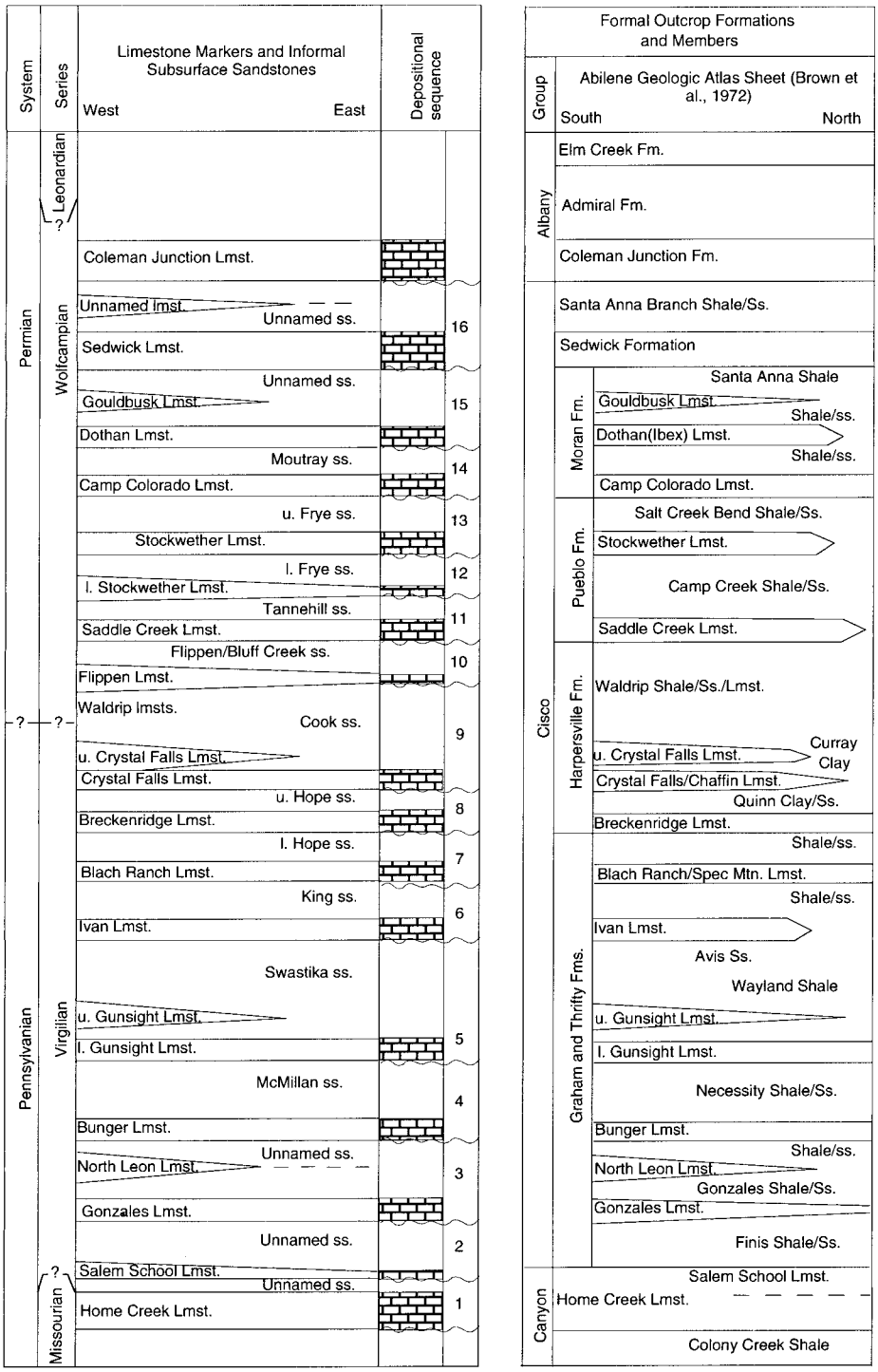

FIG. 2.—Formal and operational nomenclature, Virgilian and Wolfcampian Series, Eastern Shelf, north-central Texas. No vertical scale intended. Depositional sequences bounded by unconformities of Brown et al. (1990) are shown. Modified from Brown et al. (1990).

calculate the Cisco spectra. This method, when applied to the Milankovitch climatic series of the last 1.3 My, produced Milankovitch peaks of periods of a wider range than theoretically predicted (Yang et al. 1995). This limitation is important in spectral interpretation.

More importantly, stratigraphic incompleteness and inaccuracy in thickness–time conversion affect spectral analysis. Stratigraphic records in thickness contain erosional and nondepositional surfaces that represent time intervals (Fig. 8A, B). As a result, spectral analysis of a stratigraphic record in time, with hiatuses, is actually performed on a modified time series, where the hiatuses are ignored and segments represented by rocks are pieced together (Fig. 8C).

Thickness-to-time conversion is necessary because Milankovitch cycles are characterized in time, whereas Cisco cycles are waves in space. The conversion can be done proportionally by applying a constant sedimentation rate for the entire section (Fig. 8A, B). The spectrum of the resulting time series may or may not show indications of Milankovitch signals (e.g., Olsen 1986; Hardie et al. 1991; Yang et al. 1995). Nevertheless, because lithofacies have different sedimentation rates, the true time series of a strati-

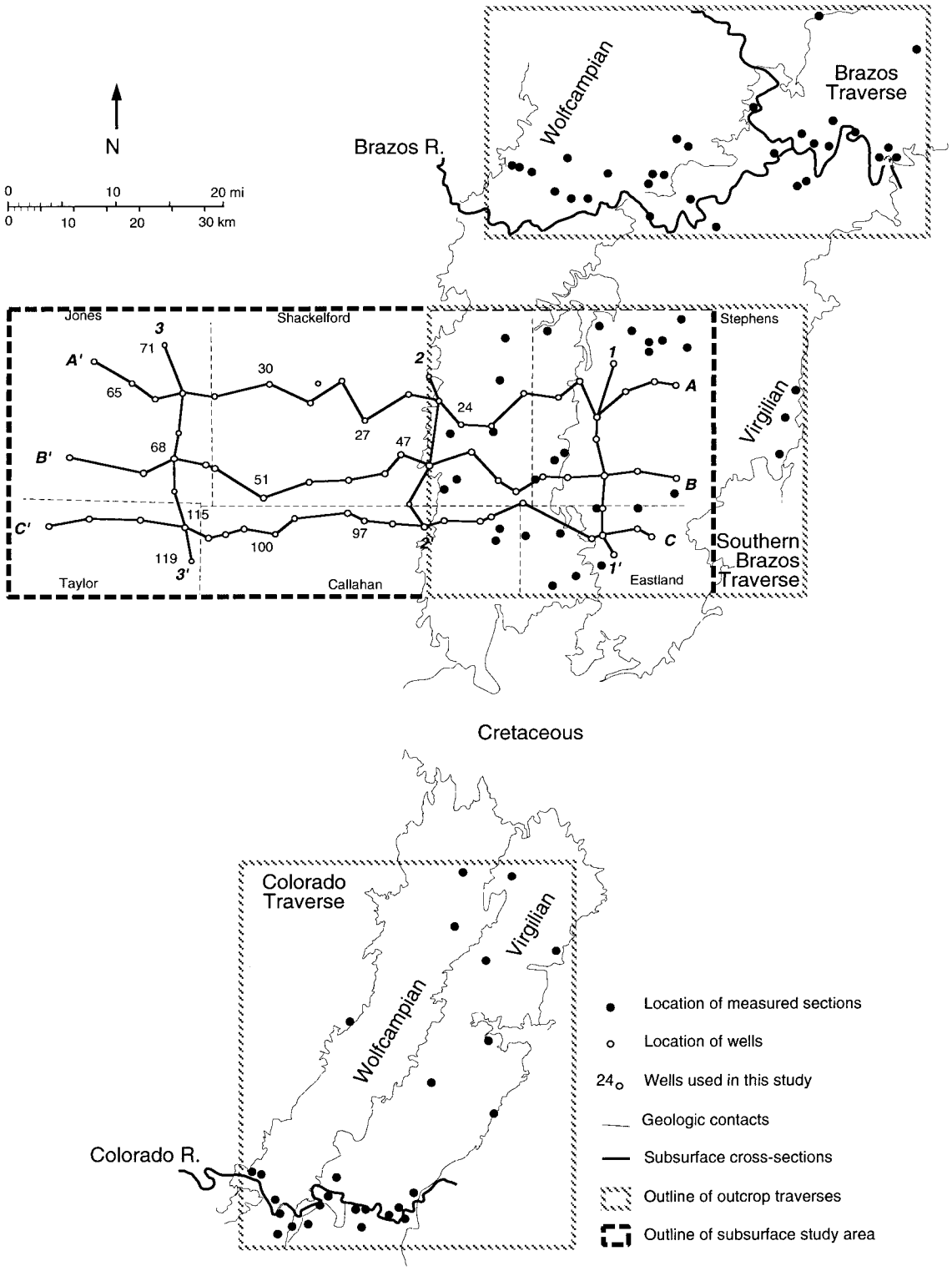

FIG. 3.—Location of outcrop sections in three traverses and wells in six cross sections on the Eastern Shelf. See Figure 1B for study areas.

graphic record will be different from the spatial series and, thus, the spectrum of the time series will also be modified (Fig. 8A, B). Although exact sedimentation rates are difficult to obtain, serious efforts have been made to achieve a more realistic thickness–time conversion (e.g., Park and Herbert 1987; Hinnov and Park 1998).

Gamma analysis of Kominz and Bond (1990) is such an effort (see also Bond et al. 1991; Kominz et al. 1991). It calculates a conversion factor, γ, for each lithofacies, which is the reciprocal of effective sedimentation rate that takes into account effects of compaction and diagenesis (Fig. 8). Assuming that the effective sedimentation rate of a lithofacies is constant

in all cycles, and that all cycles in a section have equal duration, a group of linear equations are established to calculate the γ's of individual lithofacies in a cycle:

$$T_{cy} = \sum_{i=1}^{n} \gamma_i \cdot c_{i,j} \qquad j = 1, 2, \ldots, m \tag{1}$$

where m = number of cycles, n = number of facies in a cycle, i = facies number, j = cycle number, T_{cy} = cycle period, c = facies thickness, and in reality, m is usually larger than n.

Unconstrained least-squares regression is used to solve the overconstrained linear problem in Eq 1. First, the best-fit γ's of the n facies are calculated using all m cycles. Best-fit γ's are those that minimize the variations in T_{cy}. Second, the best-fit γ's are substituted into Eq 1 to calculate the periods of the m cycles, which are different because they are calculated using fixed, best-fit γ's. ''The cycle with the largest difference from T_{cy} is removed, and the entire analysis is repeated using all the remaining cycles to calculate γ values. This procedure is continued until the number of cycles remaining is equal to the number of facies present'' (Kominz et al. 1991). In least-squares regression, both gamma assumptions are applied to calculate the best-fit γ's, but in the removal of cycles, the assumption that all cycles have equal duration is not applied. The best-fit γ's minimize the variations in period among all m cycles, but do not produce constant-period cycles (Kominz and Bond 1992).

The best-fit γ's commonly stabilize after removal of several cycles. The stabilized γ values are then used to calculate the duration of facies i in the jth cycle:

$$t_{i,j} = \gamma_i \cdot c_{i,j} \tag{2}$$

and the duration of the entire cyclic section (T) is

$$T = \sum_{j=1}^{m} \sum_{i=1}^{n} \gamma_i \cdot c_{i,j} \tag{3}$$

T includes hiatuses associated with incomplete facies in a cycle, but not hiatuses represented by entirely missed cycles (Sadler 1994).

A facies-dependent (i.e., γ-corrected) time series is converted from a section in thickness by use of Eq 2. A γ-uncorrected series is produced by applying an average γ for all lithofacies, which is calculated by dividing T in Eq 3 by the thickness of the section. Spectra of γ-corrected and uncorrected series are calculated to determine periodicity of the section and are compared with each other to determine the effects of tuning via the selected γ's.

Meaningful γ's are identified by two criteria (Bond et al. 1993). First, all γ's of all the facies must be positive at each iteration of least-squares regression. Unconstrained least-squares regression can produce negative and null γ's. They indicate failure of gamma analysis because sedimentation rates of a rock interval cannot be zero or negative, and suggest that either or both assumptions in gamma analysis are violated. That is, individual lithofacies constituting the cycles do not have approximately constant sedimentation rates, and/or the periods of cycles vary over a wide range. Thus, no positive best-fit γ's can be found to minimize the difference in duration among all the cycles. Second, a Milankovitch spectrum must be generated from the γ-corrected time series because a Milankovitch spectrum without any non-Milankovitch peaks is unique. For ancient records, in which the presence of Milankovitch signals is unknown, this criterion is replaced by less restrictive criteria (see ''DISCUSSION'') .

Gamma analysis has been applied to carbonate and siliciclastic cycles throughout the Phanerozoic (e.g., Kominz and Bond 1990; Kominz et al. 1991; Bond et al. 1991; Bond et al. 1993; Yang et al. 1995). It is effective in tuning the spectra of some cyclic strata. This study is the first application of gamma analysis to cycles composed of nonmarine to marine, mixed carbonate and siliciclastic rocks deposited during an ice-house period.

GAMMA AND SPECTRAL ANALYSES OF THE CISCO GROUP

Pre-Processing Procedures in Gamma Analysis

Two procedures are used prior to gamma analysis in this study. First, the seven facies are combined into two or three facies. For example, fluvial and delta-plain facies are combined with strandline facies as a nonmarine–marginal marine facies (Table 1). The thickness of the combined facies is the sum of the thicknesses of individual facies. Combination of facies is necessary to obtain positive and stable γ's, because many cycles do not contain all seven facies. In some cases, more than one combination scheme produces positive and stable γ's. The γ results reported here are those resulting in a maximum number of Milankovitch peaks on γ-corrected spectra.

Second, in some cases, best-fit γ's are not stable even after facies combination, and γ-corrected spectra have low resolution. This may be caused by the failure to minimize the variations in duration among all the cycles (e.g., Yang et al. 1995). The three orders of Cisco cycles probably have durations of discrete ranges (Fig. 7; Yang et al. 1998). Therefore, it is logical to group shorter-duration cycles into longer-duration cycles to minimize the difference in cycle duration before gamma analysis. Cycle grouping is somewhat arbitrary in some cases because different orders of cycles cannot always be clearly differentiated and even cycles of the same order are not of equal duration (Figs. 5, 7; Yang et al. 1998), but it does reduce variations in cycle duration. γ-corrected spectra with cycle grouping commonly display low-frequency peaks that are not present or are poorly defined on spectra without grouping. Spectral results with and without cycle grouping are compared and synthesized to delineate significant signals.

Period Calibration of Spectral Peaks

Spectral peaks are calibrated to match the Milankovitch periods. Only statistically significant peaks that coincide with peaks of the lower 90% confidence limit are calibrated. Initially, a peak is arbitrarily chosen as a Milankovitch peak, and the periods of other peaks are calibrated to it. The calibration scheme that results in a maximum number of Milankovitch peaks is achieved by trial and error, and is reported here. The calibration schemes for γ-corrected spectra with and without cycle grouping are different because the γ values are different, whereas γ-uncorrected spectra with and without cycle grouping differ only by a shift in the frequency axis, and thus their calibration schemes are the same or similar. Few exceptions exist, resulting from the effort in calibrating a maximum number of Milankovitch peaks and the fact that the uncorrected spectra with and without cycle grouping are in some cases somewhat different because of different sampling intervals in the time series.

Gamma and Spectral Results for the Outcrop Cisco Group

Spectral Results.—Five to nine peaks are calibrated on six γ-corrected spectra with and without cycle grouping (Fig. 9; Table 2). Three spectra have peaks all related to Milankovitch cycles. Two spectra have one non-Milankovitch peak. Only one spectrum has two non-Milankovitch peaks. The short-eccentricity peak is the most prominent and persistent. The short and long-obliquity peaks and the short and long-precessional index peaks are persistent. The long-eccentricity peak is the least persistent.

A peak of a period of $\sim$ 50–80 ky is present on five corrected spectra (Fig. 9). It may represent a combination tone between obliquity and precessional index cycles (see ''DISCUSSION''). The 164–222 ky peak on the corrected spectrum, with grouping, of the Colorado section may represent the long-eccentricity peak, half of which was eroded or not depos-

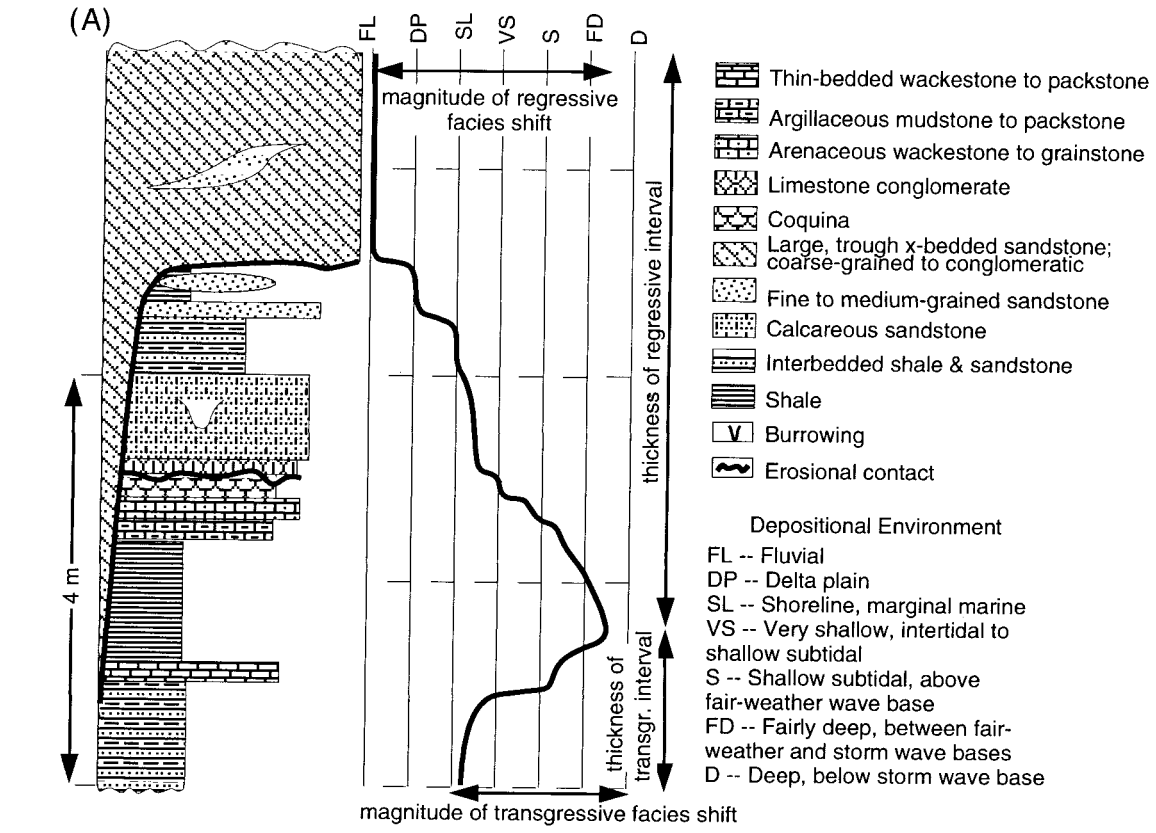
(A)
FL
DP
SL
VS
S
FD
D
magnitude of regressive facies shift
thickness of regressive interval
thickness of transgr. interval
4 m
magnitude of transgressive facies shift
Thin-bedded wackestone to packstone
Argillaceous mudstone to packstone
Arenaceous wackestone to grainstone
Limestone conglomerate
Coquina
Large, trough x-bedded sandstone; coarse-grained to conglomeratic
Fine to medium-grained sandstone
Calcareous sandstone
Interbedded shale & sandstone
Shale
Burrowing
Erosional contact
Depositional Environment
FL -- Fluvial
DP -- Delta plain
SL -- Shoreline, marginal marine
VS -- Very shallow, intertidal to shallow subtidal
S -- Shallow subtidal, above fair-weather wave base
FD -- Fairly deep, between fair-weather and storm wave bases
D -- Deep, below storm wave base

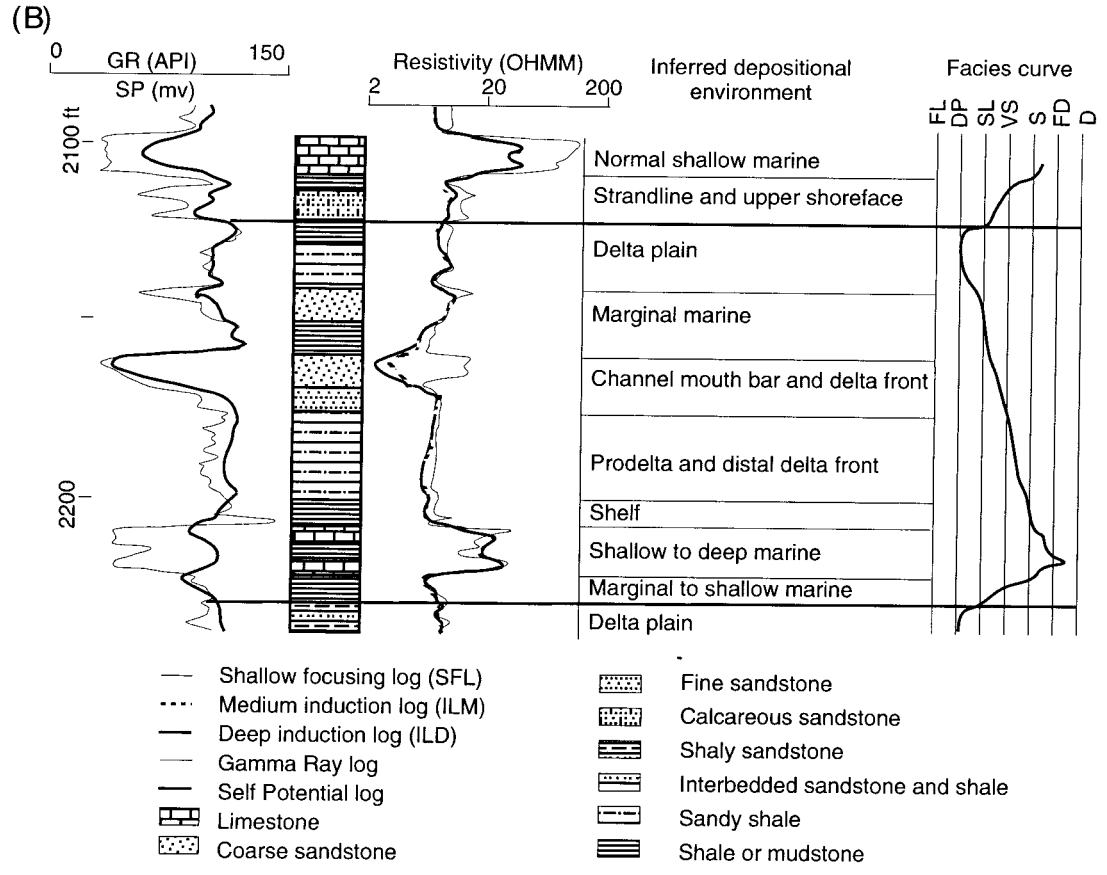
(B)
0
GR (API)
150
SP (mv)
Resistivity (OHMM)
2
20
200
Inferred depositional environment
Facies curve
FL
DP
SL
VS
S
FD
D
2100 ft
2200
Normal shallow marine
Strandline and upper shoreface
Delta plain
Marginal marine
Channel mouth bar and delta front
Prodelta and distal delta front
Shelf
Shallow to deep marine
Marginal to shallow marine
Delta plain
Shallow focusing log (SFL)
Medium induction log (ILM)
Deep induction log (ILD)
Gamma Ray log
Self Potential log
Limestone
Coarse sandstone
Fine sandstone
Calcareous sandstone
Shaly sandstone
Interbedded sandstone and shale
Sandy shale
Shale or mudstone

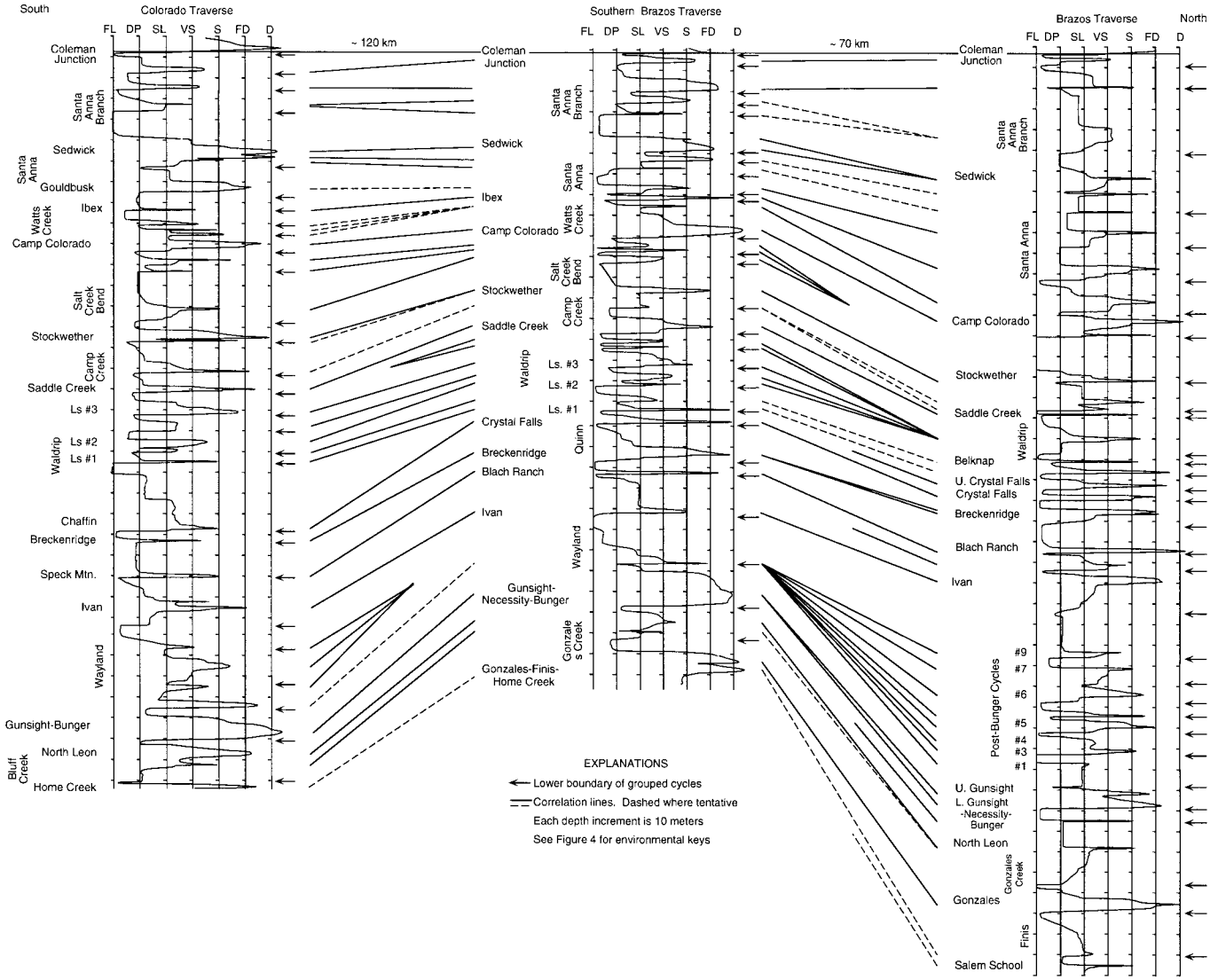

FIG. 5.—Composite outcrop sections along three traverses (Fig. 3). A composite section includes all local and regional cycles in a traverse and, thus, contains the maximum number of cycles in a traverse. If a cycle exists on several measured sections, the one in the longest section or with the largest thickness is used. Facies curves are used in quantitative analysis.

ited. The non-Milankovitch peaks are sporadic high-frequency peaks of the Colorado and southern Brazos sections (Fig. 9; Table 2).

Spectral peaks shift to higher frequency from south to north (Fig. 9). For example, the long-eccentricity peak of the Colorado section is weak in the southern Brazos section and is absent in the Brazos traverse. The shift may be related to northward increase in subsidence and sediment supply (Figs. 1, 5). Subsidence increased accommodation space, improving sediment preservation; large sediment supply recorded local transgressive–regressive events. Both factors increase stratigraphic resolution, as indicated by the large number of cycles in the Brazos section and a shift of spectral peaks toward higher frequency on all Brazos spectra.

In the least-squares regression, *Tcy* in Eq 1 is assumed to be one and has an unknown (or γ) time unit. The absolute time of a γ time unit is calculated on the basis of the Milankovitch calibration of the corrected spectra. It ranges from 33.8 to 55.3 ky (Table 3). Effective sedimentation rates are the reciprocals of γ's, and range from 7.0 to 90.1 cm/ky (Table 1). A trend of larger rates for nonmarine facies and smaller rates for marine facies agrees with the subsurface results presented later, but is disrupted by the largest rates of deep-marine facies in three records (Table 1). The large rates of deep-marine facies consisting of maximum transgressive core shale and associated deposits may be caused by continuous deposition in an offshore environment. But the large variations of gamma-derived rates for this and other facies indicate that the rates may not be regarded as true sedimentation rates because of variable schemes of facies combination and

←

FIG. 4.—Cycle delineation in **A)** outcrop and **B)** subsurface. Subsurface facies interpretation and cycle delineation are based on outcrop anologs and about 5000 ft core calibration of wireline logs. Environmental interpretations are displayed as facies curves on a grid. Cycle magnitude and thickness are also defined.

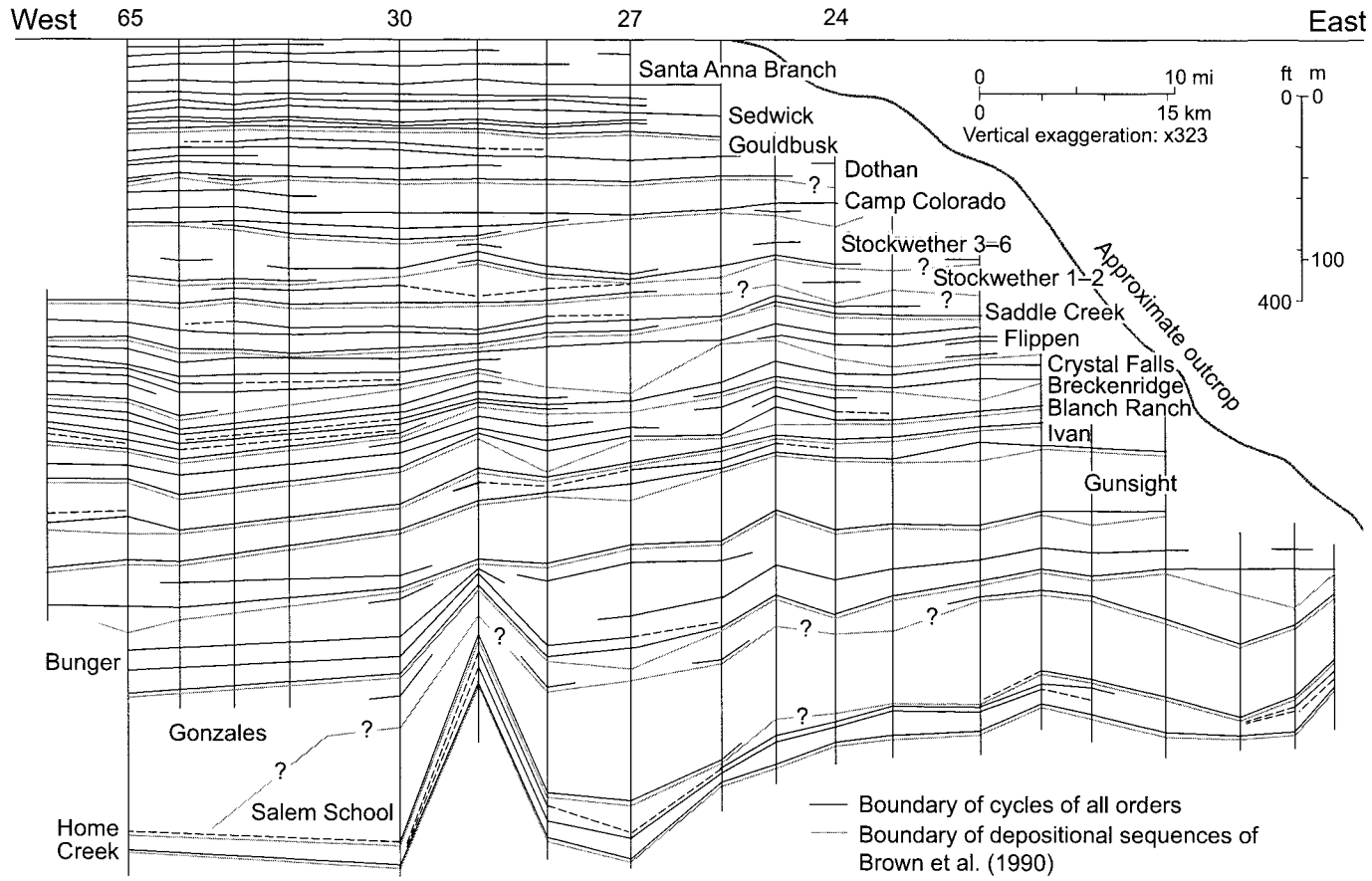

FIG. 6.—Simplified dip stratigraphic cross section A–A′ showing shelf configuration and systematic changes of cycle abundance, continuity, and thickness. See Figure 3 for location.

cycle grouping, and the relative magnitude of these rates should be emphasized instead. Moreover, the duration of each record (T) is calculated from Eqs 2 and 3, ranging from 1007 to 1532 ky (Table 3). The average effective sedimentation rate of a section is calculated by dividing the total thickness by T (Table 1). It ranges from 23.7 to 44.0 cm/ky.

The duration of the Cisco Group is also estimated as 14 My and 17 My using the time scales of Klein (1990) and Harland et al. (1989), respectively, assuming that the thickness of Cisco Group is proportional to the duration of the Virgilian and Wolfcampian series (Yang 1995). If the γ-estimated duration is represented by rocks and the chronostratigraphic estimates are correct, only $\sim$ 6 to 11% of the Cisco time is represented by rocks. Assuming that the 16 regional unconformities in the Cisco Group represent the missing time, their average duration ranges from $\sim$ 780 to 1000 ky (Fig. 2; Brown et al. 1990). Finally, the Brazos section, which is the thickest and contains the largest number of cycles among the three sections, has the shortest depositional duration (Fig. 5; Table 3). This is probably because of the large amount of nonmarine and shallow-marine siliciclastic facies and the small amount of carbonate and deep-marine facies in this section (Lee 1938; Brown et al. 1990; Yang 1995, 1996). The nonmarine and shallow-marine siliciclastic facies generally have higher sedimentation rates, and thus represent less time per unit of thickness than the carbonate and deep-marine facies, as indicated by the large average effective sedimentation rate of this section (Table 1). As a result, the Brazos section, although thicker than the Colorado and Southern Brazos sections, has the shortest depositional duration.

Gamma and Spectral Results of the Subsurface Cisco Group

Spectral Results.—Five to nine peaks are calibrated on 24 γ-corrected spectra with and without cycle grouping (Fig. 10A, B; Table 2). Twelve spectra have peaks all related to Milankovitch cycles. Nine spectra have one non-Milankovitch peak. Only three spectra have two non-Milankovitch peaks. The Salem School cycle is excluded in gamma and spectral analyses, because it is extremely thick and contains deep marine anoxic shale, which is absent in the other cycles (Fig. 7; Brown et al. 1990).

The short-eccentricity peak is the most prominent and persistent. The long-eccentricity peak is persistent and is prominent on some spectra, but is absent on six spectra without cycle grouping. The wide period range of this peak is caused, at least partially, by the low precision at the low-frequency band, because only few long-period cycles are present in the series.

The short-obliquity and long-obliquity peaks (34.3 ky and 42.9 ky) are persistent. In some cases, the long-obliquity peak has higher magnitude than the short-obliquity peak. This could be caused by (1) the increase of red noise toward low frequency, such as in section B–B′, or (2) a tendency for the long-obliquity peak to merge with an adjacent lower-frequency peak, resulting in higher magnitude, such as in some spectra of section C–C′ (Fig. 10A, B).

The precessional index peaks are calibrated on 12 spectra and are less persistent than the eccentricity and obliquity peaks. They are more common in the up-dip sections (e.g., section C–C′). This is unexpected because of the relatively low stratigraphic resolution in the up-dip sections (Figs. 6,

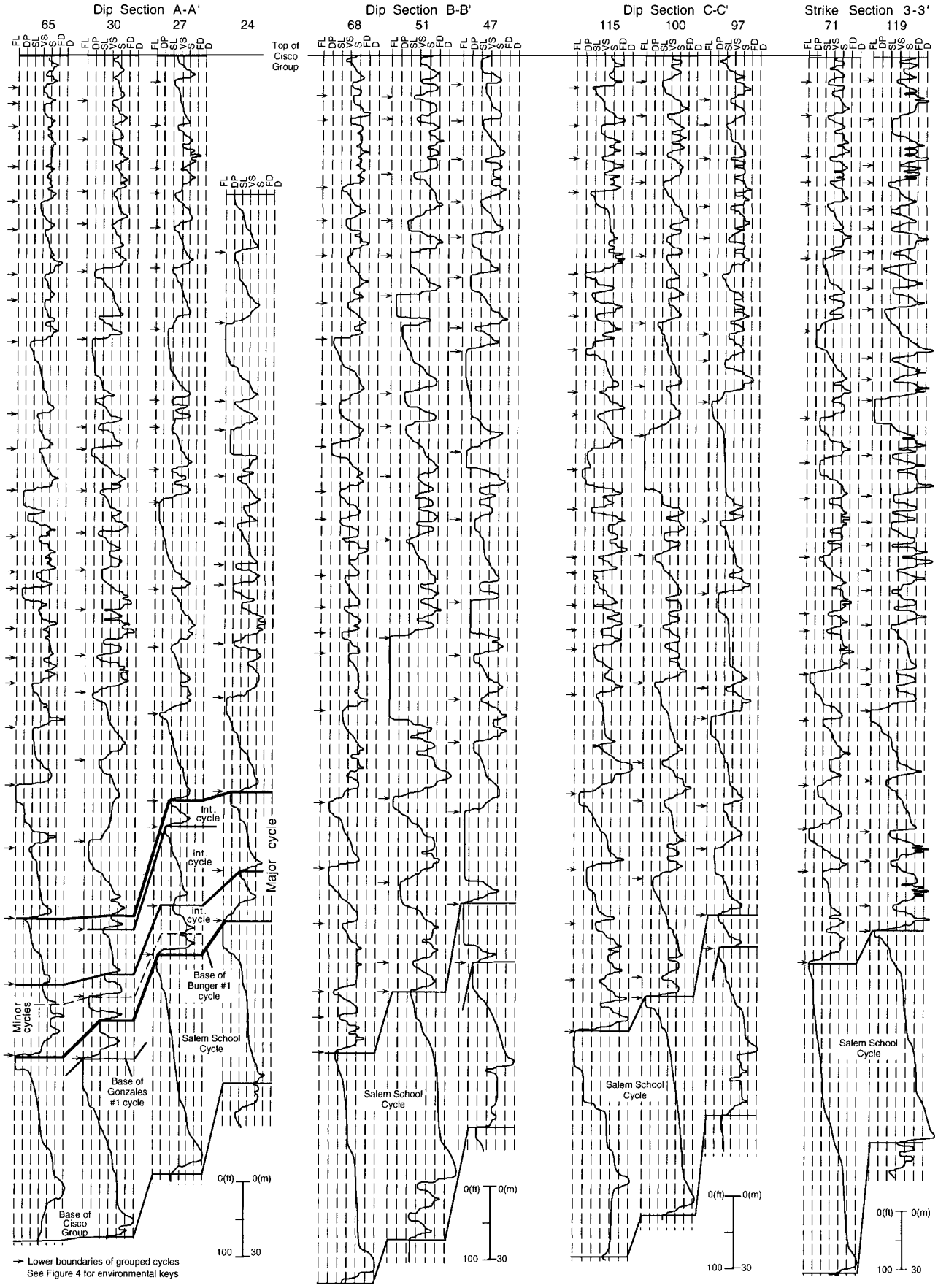

FIG. 7.—Facies curves of wells in dip sections A–A′, B–B′, and C–C′, and strike section 3–3′, which are used in quantitative analysis. The relationship among major, intermediate, and minor cycles is demonstrated on A–A′. Location of sections and wells is shown in Figure 3.

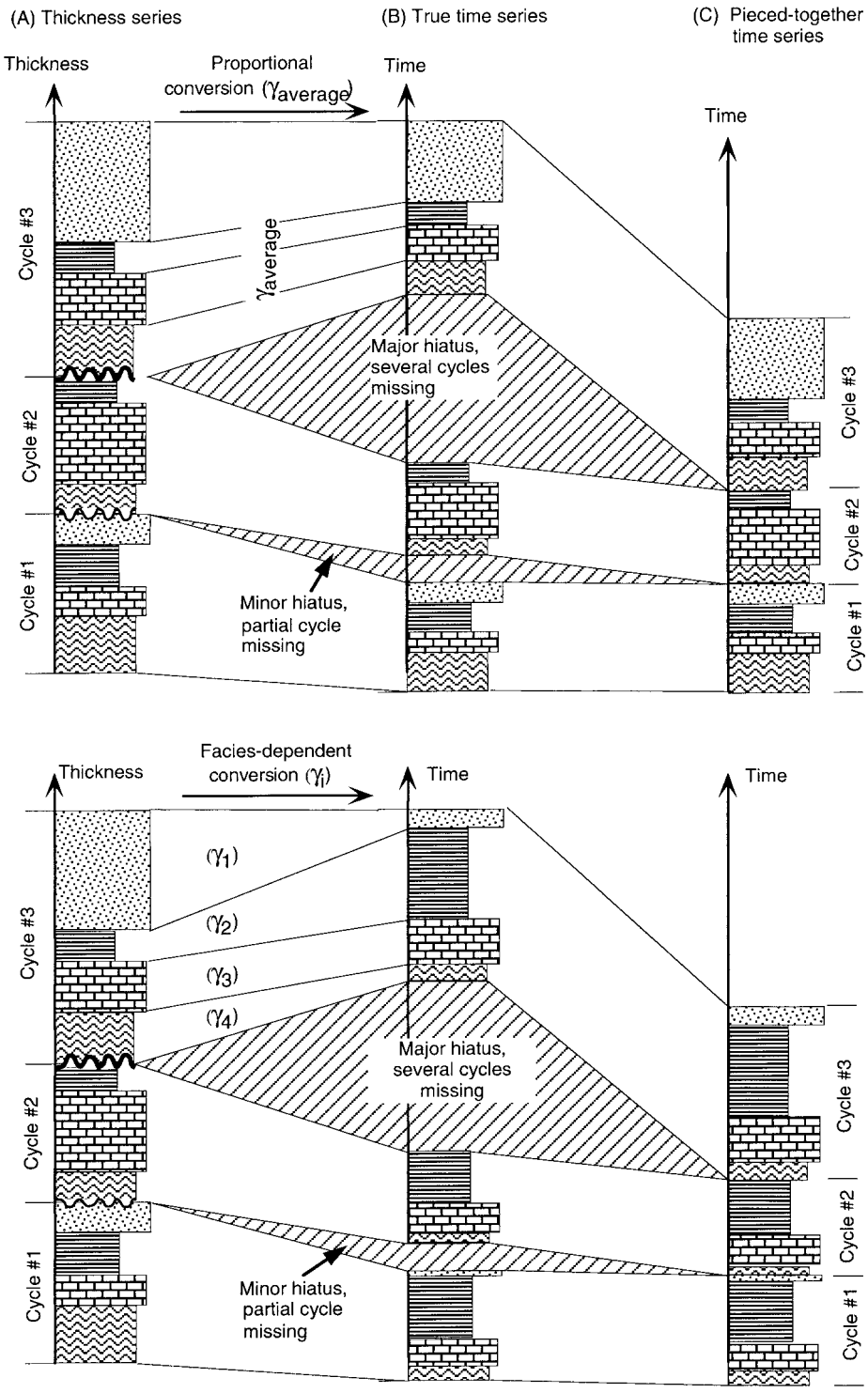

FIG. 8.—Diagram showing thickness-to-time conversion [(A) to (B)]. The conversion is proportional (A to B, upper part) or facies dependent (A to B, lower part). Intervals represented by rocks are pieced together to construct time series for spectral analysis (C).

7; Yang et al. 1998). Moreover, commonly a precessional index peak is calibrated on the spectrum without cycle grouping but not on that with cycle grouping.

Other possible Milankovitch-related peaks include those of a period varying from 50 to 80 ky and those of a period of ~ 200 ky. The former is persistent but not well defined. It is, in some cases, well defined and prominent on γ-corrected spectra without cycle grouping (Fig. 10A, B). The 200 ky peak is poorly to moderately defined and not persistent (Fig. 10A, B).

Non-Milankovitch peaks are sporadic and poorly defined. The low-frequency ones have periods varying from 600 to 1700 ky. The high-frequency ones have periods of ~ 25 ky or smaller than 16 ky, and are present only on γ-corrected spectra without cycle grouping. Some may represent poorly tuned short-precessional index peaks (e.g., Well 47).

TABLE 1.—*Selected best-fit γ's (γ time/m in outcrop, γ time/ft in subsurface), effective sedimentation rates of various facies, and average effective sedimentation rates of the Cisco sections.*

			Selected best-fit γs							Effective sedimentation rates (cm/ky)							Average effective sedimentation rates (cm/ky)
			nonmarine	nonmarine & marg. marine	marginal marine	marginal & shallow marine	shallow marine	shallow & deep marine	deep marine	nonmarine	nonmarine & marg. marine	marginal marine	marginal & shallow marine	shallow marine	shallow & deep marine	deep marine	
Outcrop comp. sections	Colorado	w/o gr.	0.040		0.158		0.383		0.030	66.9		17.0		7.0		90.1	29.0
		w/ gr.	0.059			0.099			0.108	30.5			18.2			16.7	23.7
	south. Brazos	w/o gr.		0.096			0.019		0.029		27.0			13.7		88.3	25.4
		w/ gr.		0.071			0.166		0.025		27.4			11.7		77.4	24.2
	Brazos	w/o gr.	0.051			0.121			0.229	57.7			24.4			12.9	39.2
		w/ gr.	0.034			0.070			0.217	68.0			32.6			10.6	44.0
Dip section A-A'	24	w/o gr.		0.007				0.034			71.0				14.6		41.0
		w/ gr.		0.011				0.014			41.6				30.3		38.9
	27	w/o gr.		0.006			0.015		0.074		122.9			53.7		10.7	44.3
		w/ gr.		0.009				0.026			61.3				21.3		41.0
	30	w/o gr.		0.013			0.026		0.053		49.6			24.0		12.0	24.9
		w/ gr.		0.008				0.021			39.9				15.0		25.1
	65	w/o gr.		0.008				0.042			54.5				10.6		19.0
		w/ gr.	0.009		0.032			0.021		34.2		10.0			15.5		19.5
Dip section B-B'	47	w/o gr.		0.006			0.018		0.040		77.5			26.3		11.6	29.9
		w/ gr.	0.007		0.034			0.018		51.3		10.8			20.5		30.0
	51	w/o gr.	0.002		0.028			0.028		229.8		17.2			16.9		24.4
		w/ gr.		0.008				0.016			33.0				17.4		25.1
	68	w/o gr.		0.008				0.055			63.2				8.8		19.6
		w/ gr.	0.012		0.028			0.009		29.4		12.0			39.7		24.1
Dip section C-C'	97	w/o gr.	0.002			0.032			0.053	246.2			14.4			8.7	24.9
		w/ gr.		0.006				0.028			66.6				14.8		34.4
	100	w/o gr.		0.001				0.057			540.0				9.5		25.1
		w/ gr.		0.002				0.022			119.6				12.0		27.9
	115	w/o gr.		0.007			0.029		0.038		80.5			18.3		13.6	24.5
		w/ gr.		0.013				0.018			30.1				20.8		25.5
Strike sec. 3-3'*	71	w/o gr.		0.002				0.048			220.0				9.6		19.4
		w/ gr.		0.008				0.016			25.3				12.9		18.7
	119	w/o gr.		0.006				0.058			89.7				9.2		19.4
		w/ gr.		0.010			0.022		0.025		35.2			16.3		14.2	20.8

* Wells 68 and 115 of strike section 3-3′ are listed in dip sections B-B′ and C-C′.

The non-Milankovitch peaks likely represent random components in the Cisco records.

The γ-uncorrected spectra contain relatively low-magnitude peaks (Fig. 10C, D). Many peaks could be noise and, thus, period calibration is uncertain at best. Nevertheless, many statistically significant peaks have periods similar to those on the γ-corrected spectra.

Gamma Results and Sedimentation Rates.—γ's of the combined facies have consistent relative magnitude, and are more stable than those of the outcrop cycles (Fig. 11A, B; Table 1). γ-estimated effective sedimentation rates show some consistent trends: (1) nonmarine facies and combined nonmarine and marginal-marine facies have higher rates than combined shallow-marine facies and deep-marine facies, and other individual

facies, (2) deep-marine facies and, in most cases, combined deep-marine and shallow-marine facies have lower rates than other individual and combined facies, and (3) marginal-marine facies have very low rates. These trends also exist in many trials not reported here. Sedimentation rates of individual facies range from 8.8 to 540.0 cm/ky, and average sedimentation rates range from 19.0 to 44.3 cm/ky (Table 1).

The absolute time of a γ time unit (i.e., T_{cy}) ranges from 38.5 to 69.1 ky without cycle grouping, and from 55.3 to 114.3 ky with grouping (Table 3). Least-squares regression minimizes the difference in duration among all the cycles. Therefore, the time of a γ time unit represents, to some degree, the least-squares mean duration of the cycles. Cycle grouping increases the mean duration and, thus, the unity of γ time. The wide range is caused by variable calibration frequencies of γ-corrected spectra with and without grouping for wells distributed over a large area.

γ-Estimated Duration.—The duration of Cisco records increases systematically from 798 to 2658 ky in the down-dip direction (Table 3). The down-dip sections represent about twice as much time as the up-dip ones, although they are not much thicker (Fig. 7). The down-dip increase in duration is probably caused by down-dip increase of cycle abundance and thickness of marine facies (Figs. 6, 7; Yang et al. 1998). Marine facies generally have lower sedimentation rates and represent more time than nonmarine facies, as indicated by overall decrease of effective sedimentation rates in down-dip sections (Table 1).

The duration of entire Cisco Group including the Salem School cycle ranges from 1479 to 3440 ky (Table 3). The duration of the Salem School cycle is calculated using the average sedimentation rate. The ratio of the γ-estimated duration to the chronostratigraphic estimates indicates that only $\sim$ 7 to 25% of the Cisco time is represented by rocks.

DISCUSSION

Validity of Gamma Results of the Cisco Group

Thickness–time conversion by γ's generated more realistic time series and spectra. This is indicated by: (1) the positive and stable γ's, (2) the consistency of relative magnitude of γ's of various facies, and (3) the improved resolution and Milankovitch calibration of γ-corrected spectra.

Positive γ's in all 30 gamma analyses indicate that gamma analysis and the procedures of facies combination and cycle grouping are reasonable. In most cases, γ's stabilize after removal of a few anomalous cycles. This indicates that the assumption that facies have unique sedimentation rates is not violated, and that variations in duration among cycles used in gamma analysis are small enough to be minimized through least-squares regression.

γ values of various facies display consistent trends in the study area (Fig. 4; Table 1), and effective sedimentation rates agree with those of many ancient and modern sediments (Enos 1991; Wilkinson et al. 1992; Sadler 1994). In general, gamma analysis has obtained different sedimentation rates for different facies. Therefore, the γ-corrected time series should be more realistic than the uncorrected ones.

The validity of γ conversion is further supported by improved resolution of γ-corrected spectra. γ tuning commonly splits a broad peak on the uncorrected spectrum into two or more distinct peaks. In few cases, γ tuning eliminates Milankovitch peaks on the uncorrected spectra (e.g., the spectra without grouping of Well 65), or produces non-Milankovitch peaks not present on the uncorrected spectra (e.g., the spectra without grouping of Well 24 and the southern Brazos spectra) (Figs. 9, 10A, C). In general, however, γ tuning makes major Milankovitch-related peaks more distinct and greatly reduces the background noise (Fig. 10). This is most evident in down-dip wells.

Lastly, forward modeling of a Plio-Pleistocene deep-sea gray-scale record suggests that successful γ tuning should produce a spectrum with more precisely defined Milankovitch peaks in an orbitally controlled record (Kominz 1996). In this study, the improved resolution produces more Milankovitch-related peaks on γ-corrected spectra than on the uncorrected spectra, suggesting successful γ tuning (Figs. 9, 10).

Validity of the Spectral Results of the Cisco Group

The validity of spectral results is indirectly indicated by: (1) systematic down-dip increase of γ-estimated duration of the Cisco Group, (2) similar Milankovitch peaks calibrated on both γ-corrected and γ-uncorrected spectra of a record, and (3) reasonable and consistent sedimentation rates.

The γ-estimated Cisco duration increases systematically in the down-dip direction over a distance of $\sim$ 100 km on the shelf (Fig. 3; Table 3). This is in accordance with the down-dip increase in cycle abundance and thickness of marine facies (Fig. 6; Yang et al. 1998). In addition, the durations of a series with and without grouping are similar, although calibration schemes are different. Furthermore, series along depositional strike have similar duration (Table 3). The above facts indicate that the simple and arbitrary gamma assumptions and calibration schemes are consistent with geological expectations.

Similar Milankovitch peaks are commonly calibrated on corresponding γ-corrected and uncorrected spectra. Generally, the spectra have different configurations, and peaks on the uncorrected spectra are poorly defined. However, the similar periods of many prominent and/or persistent peaks on both spectra suggest that the Milankovitch calibration is not artificial.

Finally, the sedimentation rates calculated on the basis of the Milankovitch calibration are comparable with those of many ancient and Recent analogs, suggesting that the Milankovitch calibration of gamma time scales is reasonable.

Possible Miscalibration of the Cisco Spectra

Milankovitch calibration of the Cisco spectra may be inappropriate, as indicated by: (1) some inconsistency in facies combination and some arbitrariness in cycle grouping, (2) presence of non-Milankovitch peaks on γ-corrected spectra, and (3) discrepancy between γ-estimated and chronostratigraphic duration of the Cisco Group.

Five schemes of facies combination are used to produce positive and stable γ's. The schemes for some sections with and without cycle grouping are different. Cycle grouping uses variable cutoffs, although efforts are made to group minor cycles into intermediate cycles (Figs. 5, 7). Strong white noise is indicated by numerous high-frequency to medium-frequency peaks on the spectra without grouping of wells 97 and 100 (Fig. 10A). γ tuning with grouping reduces white noise by eliminating some high-frequency peaks but increases the red noise (e.g., Brazos section, wells 97 and 100; Figs. 9, 10A, B). Red noise makes calibration difficult for some peaks (e.g., the 103–137 ky peak on the spectrum with grouping of Well 51; Fig. 10B).

However, statistically significant peaks are readily identified. Given the complex facies variations and the presence of three orders of cycles, the effective sedimentation rates are reasonably consistent and within the range of many ancient and Recent analogs. The corrected spectra have much

→

FIG. 9.—γ and spectral results of outcrop composite sections displayed in three columns. **A, B)** γ results with and without cycle grouping. **C–F)** Spectral results with and without grouping for γ-corrected and -uncorrected series. Thick lines are the spectra; thin lines are the lower 90% confidence limits; numbers above peaks are periods in ky; bold italic numbers are initial calibration periods; horizontal bar above a peak indicates the period range; vertical bars on the frequency axes are Milankovitch line spectra at 300 Ma. f_n is the Nyquist frequency. See text for discussion.

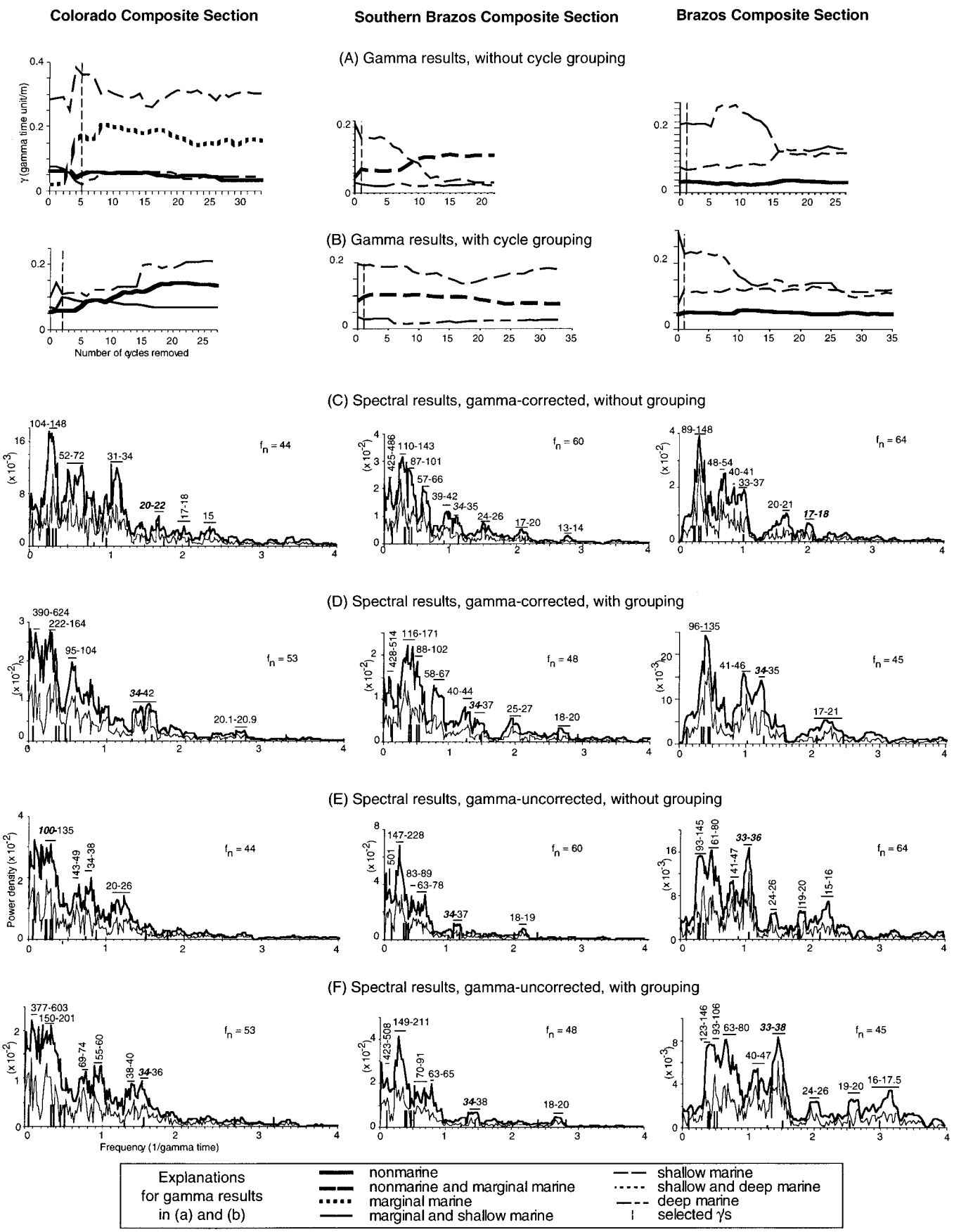
Colorado Composite Section
Southern Brazos Composite Section
Brazos Composite Section
(A) Gamma results, without cycle grouping
(B) Gamma results, with cycle grouping
γ (gamma time unit/m)
Number of cycles removed
(C) Spectral results, gamma-corrected, without grouping
(D) Spectral results, gamma-corrected, with grouping
(E) Spectral results, gamma-uncorrected, without grouping
(F) Spectral results, gamma-uncorrected, with grouping
Power density
Frequency (1/gamma time)
Explanations for gamma results in (a) and (b)
nonmarine
nonmarine and marginal marine
marginal marine
marginal and shallow marine
shallow marine
shallow and deep marine
deep marine
selected γs

TABLE 2.—*Spectral results of γ-corrected spectra of the Cisco Group.*

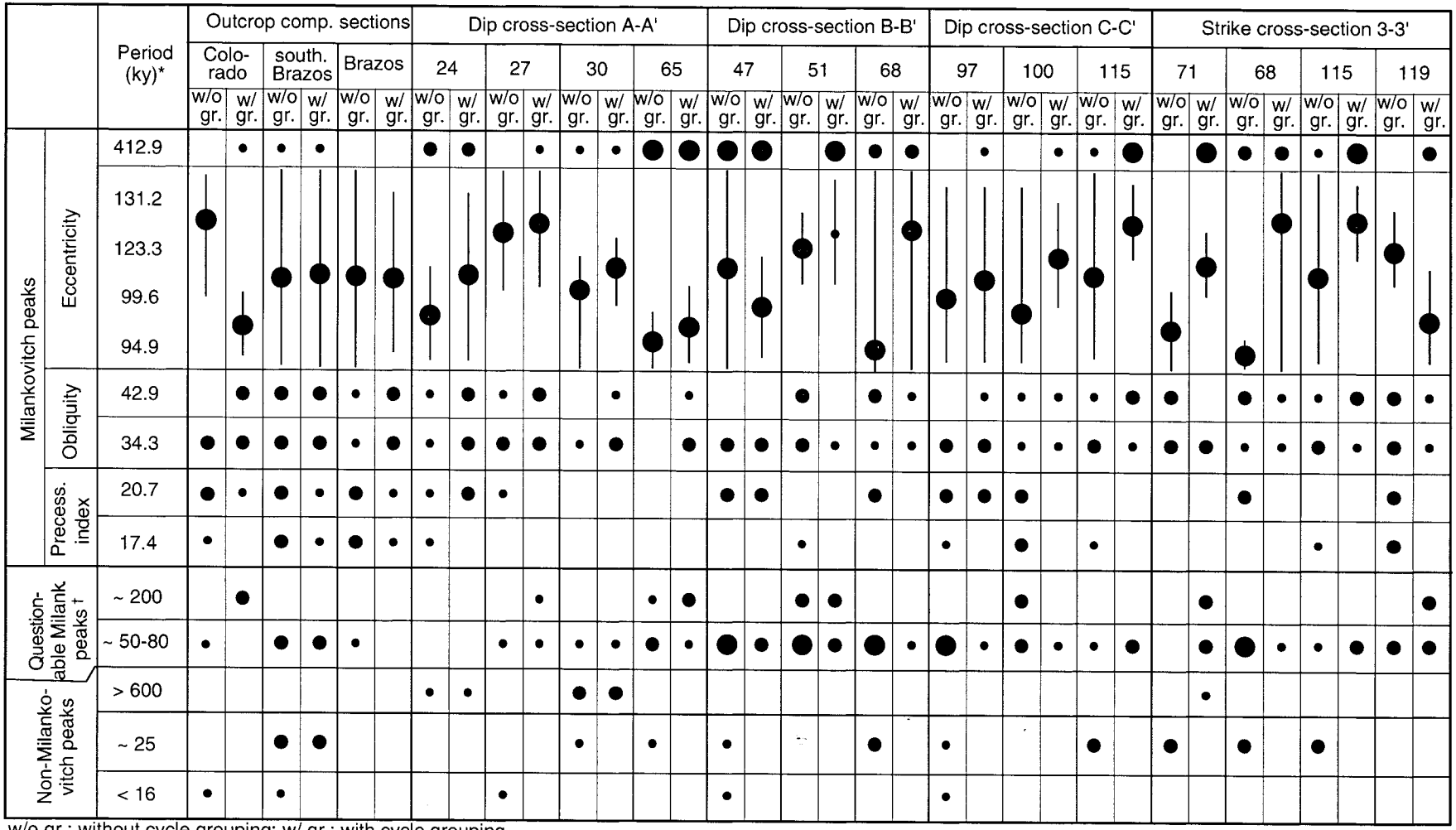

w/o gr.: without cycle grouping; w/ gr.: with cycle grouping

● - Statistically significant, prominent peaks; ● - Statistically significant, well-defined peaks; • - Statistically significant, fairly well-defined or poorly defined peaks; "blank"- No peaks are calibrated. Vertical bar through filled circles indicates the range of calibrated periods of short-eccentricity peaks.

* Periods of Milankovitch cycles at 300 ma from Berger et al. (1992).

† ~ 200-ky period may be the half of long-eccentricity period; ~50-80-ky period may be a combination tone -- $1/(f_3 - f_1 + f_2)$, where f_1, f_2, and f_3 are the frequencies of short and long precessional index and short obliquity cycles. See text for discussion.

TABLE 3.—*Duration of the unit of γ time scales, duration of the Cisco records used in gamma and spectral analyses, duration of the Salem School cycle, and duration of the entire Cisco Group.*

			Unity of gamma time scale (ky)	Duration of record used (ky)	Duration of Salem School Cycle (ky)	Duration of entire Cisco Group (ky)
Outcrop comp. sections	Colorado	w/o gr.	37.3	1247		1247
		w/ gr.	55.3	1532		1532
	south. Brazos	w/o gr.	38.5	1211		1211
		w/ gr.	51.6	1274		1274
	Brazos	w/o gr.	33.8	1111		1111
		w/ gr.	43.3	1007		1007
Dip section A-A'	24	w/o gr.	61.8	798	223	1021
		w/ gr.	69.5	841	234	1057
	27	w/o gr.	38.5	942	207	1149
		w/ gr.	55.3	1016	223	1239
	30	w/o gr.	48.0	1790	306	2096
		w/ gr.	96.4	1776	304	2080
	65	w/o gr.	69.1	2274	352	2626
		w/ gr.	94.5	2208	352	2560
Dip section B-B'	47	w/o gr.	65.6	1333	153	1486
		w/ gr.	83.3	1327	152	1479
	51	w/o gr.	63.6	1670	325	1995
		w/ gr.	112.3	1624	316	1940
	68	w/o gr.	62.0	2271	482	2753
		w/ gr.	90.0	1840	392	2232
Dip section C-C'	97	w/o gr.	65.3	1560	220	1780
		w/ gr.	73.7	1129	159	1288
	100	w/o gr.	55.9	1648	279	1927
		w/ gr.	111.9	1483	251	1734
	115	w/o gr.	58.3	1786	423	2209
		w/ gr.	79.9	1717	406	2123
Strike section 3-3'	71	w/o gr.	66.4	2562	754	3316
		w/ gr.	114.3	2658	782	3440
	68	w/o gr.	62.0	2271	482	2753
		w/ gr.	90.0	1840	392	2232
	115	w/o gr.	58.3	1786	423	2209
		w/ gr.	79.9	1717	406	2123
	119	w/o gr.	57.2	2187	534	2721
		w/ gr.	85.1	2037	498	2533

higher resolution than the uncorrected spectra, which increases in downdip wells, corresponding to the increase in stratigraphic resolution (Fig. 10A, B). The above evidence suggests that the inconsistencies in facies combination and cycle grouping are secondary.

The presence of non-Milankovitch peaks on corrected spectra suggests that some other calibration schemes could produce other sets of non-Milankovitch and Milankovitch peaks. But any other schemes generate fewer Milankovitch peaks, which commonly have peculiar magnitude relations irreconcilable with the theoretically predicted relations, such as a prominent long-obliquity peak and a weak short-eccentricity peak (Berger 1988). More significantly, the adapted schemes result in consistent age relations among all sections and reasonable sedimentation rates, suggesting optimal choices.

Finally, the ratio between the γ-derived and the chronostratigraphic duration of the Cisco Group suggests that ~ 75–94% of the Cisco time is not represented by rocks. The amount of time is significant but possible (e.g., Wilkinson et al. 1992; Yang et al. 1995). The 16 unconformities across the shelf may well represent the missing time. The duration of sea-level lowstand deposits basinward of the shelf edge is estimated on the basis of the progradational thickness of these deposits and the average sedimentation rate of the shelf deposits (Fig. 1C). It is approximately equal to the missing time of the Cisco Group on the shelf, indicating that the γ-derived duration is a reasonable estimate of the depositional duration on the shelf.

Origin of Depositional Cyclicity of the Cisco Group

The dominance of Milankovitch-related peaks on the Cisco spectra suggests that the Cisco cyclicity is closely related to Milankovitch climatic cycles. The predominance of the short-eccentricity peak and the persistence of long-eccentricity and short-obliquity peaks suggest that they are more robust than precessional index cycles (Figs. 9, 10A, B; Table 2). Short-eccentricity cycles probably exerted the dominant control on Cisco cycles; the influence of long-eccentricity and obliquity cycles was also significant, whereas that of precessional index cycles was minor.

Results of geologic analysis of the Cisco Group support the above interpretation. Average cycle period and stacking patterns of the outcrop cycles suggest an ambiguous but possible match with eccentricity and obliquity cycles (Yang 1995). Analysis of cycle symmetry suggested major eustatic control on accommodation space and major climatic control on sediment yield and supply (Yang 1996). Cycle correlation identified three orders of cycles (Yang et al. 1998). Regional ordered transgressive–regressive events and systematic changes of cycle character indicate that Milankovitch climatically controlled eustasy was the major control on cyclic sedimentation of nonmarine and marine carbonate and siliciclastic facies.

Late Paleozoic time was a period of active continental glaciation similar to that of the Plio-Pleistocene (Crowell 1978; Imbrie and Imbrie 1979; Berger 1988; Veevers and Powell 1987). Many studies of Late Paleozoic cycles in North America have suggested Milankovitch-related eustasy as the dominant control on cycle formation (e.g., Wanless and Shepard 1936; Wilson 1967; Heckel 1977, 1986; Connolly and Stanton 1992; Goldhammer et al. 1994; Soreghan 1994). High-frequency eustatic control has also been suggested for the Cisco cycles (e.g., Lee 1938; Harrison 1973; Boardman and Malinky 1985; Boardman and Heckel 1989; Brown et al. 1990; Yancey 1991). The results of this study strongly support these speculations.

Subtropical and tropical African paleoclimatic changes of the last 5 My are interpreted from wind-borne dust variability in offshore West and East Africa (deMenocal 1995) and are analogous to those in the Eastern Shelf region in Virgilian and Wolfcampian time (Fig. 3). African terrestrial climate variability has shifted in accordance with changes in high-latitude glacial climate (deMenocal 1995). Before 2.8 Ma African climate varied

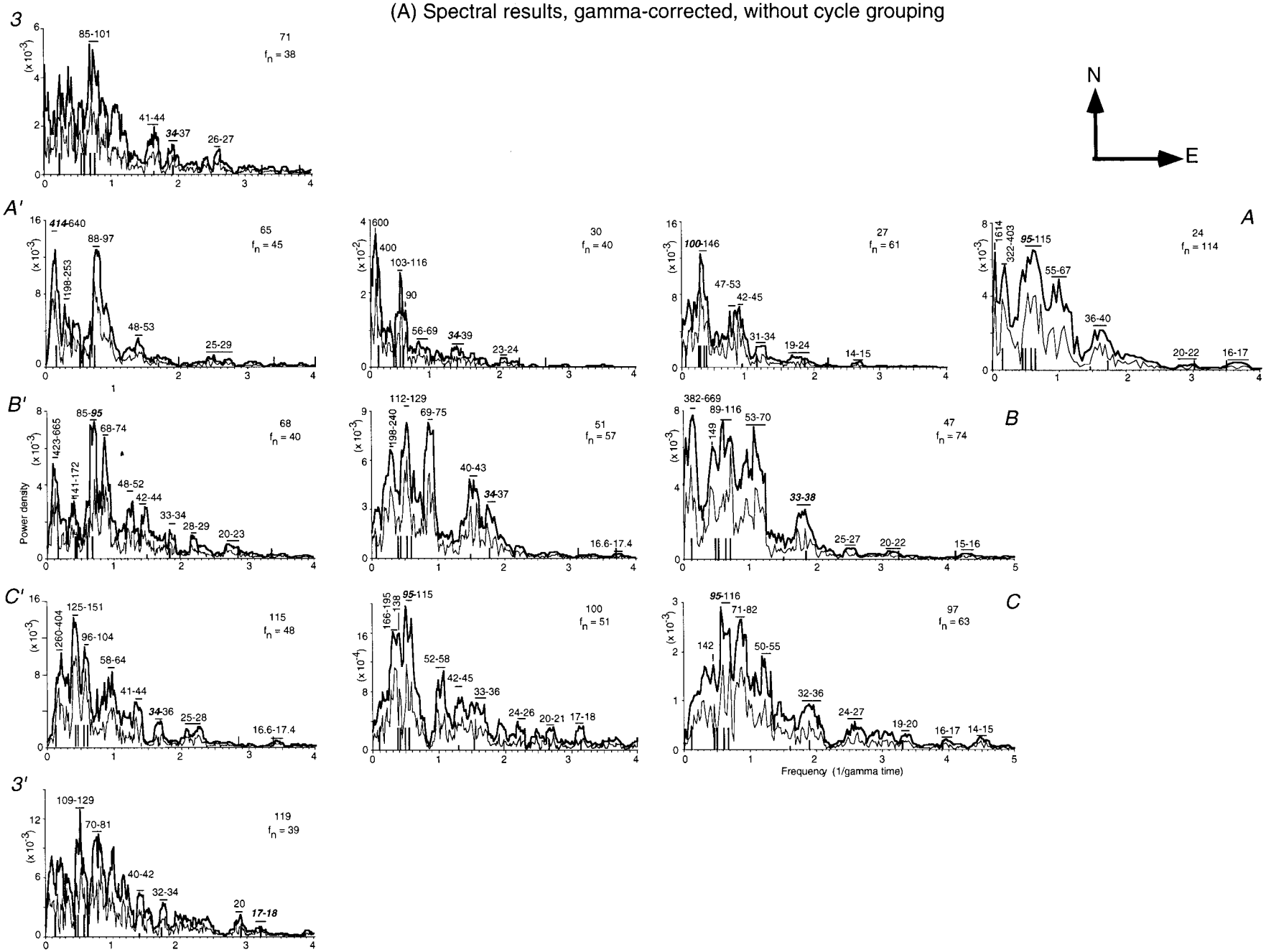

FIG. 10.—Spectral results of subsurface sections: **A, B)** γ-corrected without and with cycle grouping, **C, D)** γ-uncorrected without and with grouping. Spectra are arranged with respect to locations of the sections (Fig. 3). See Figure 9 for keys to the spectra. See text for discussion.

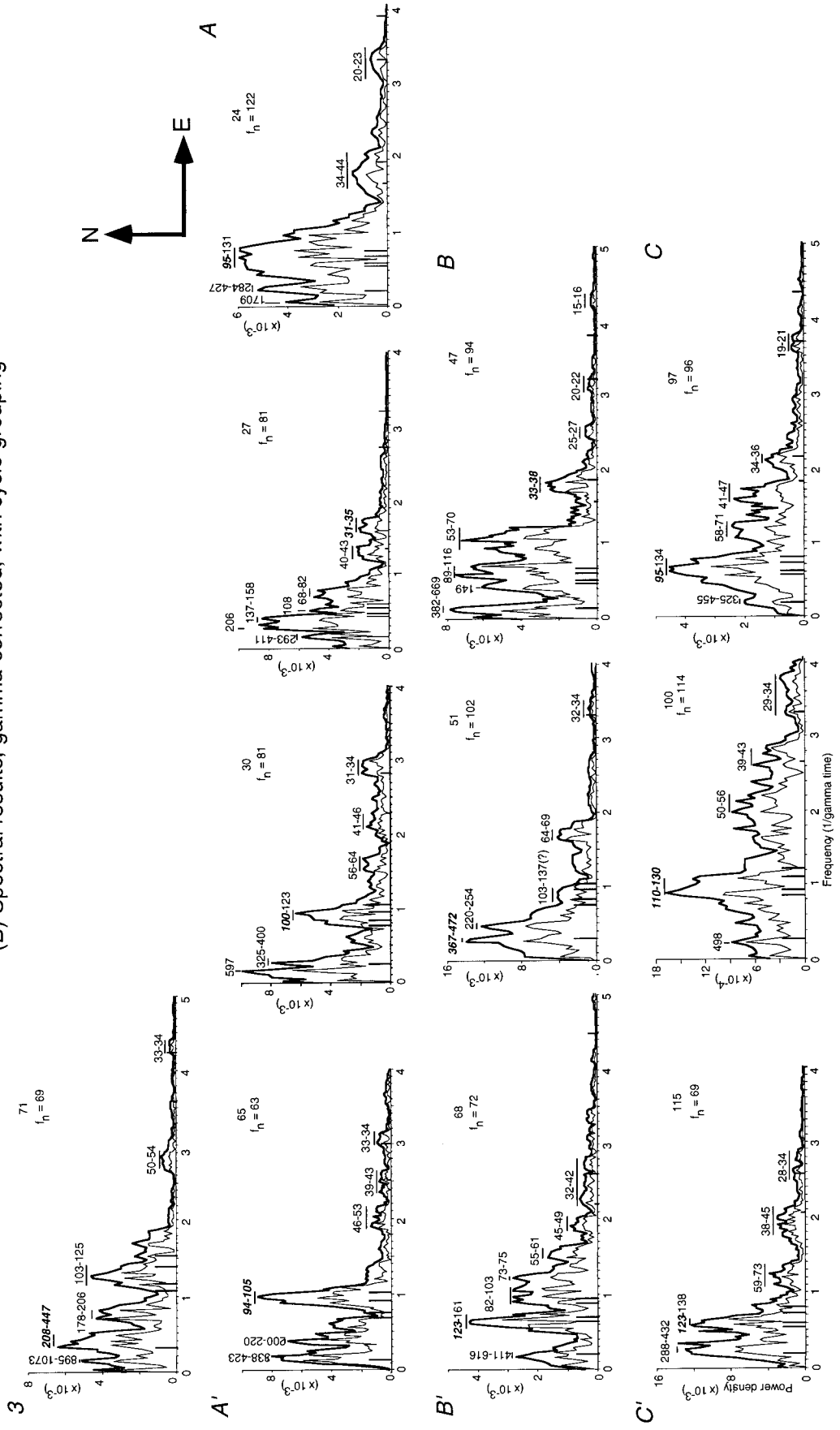

FIG. 10.—Continued.

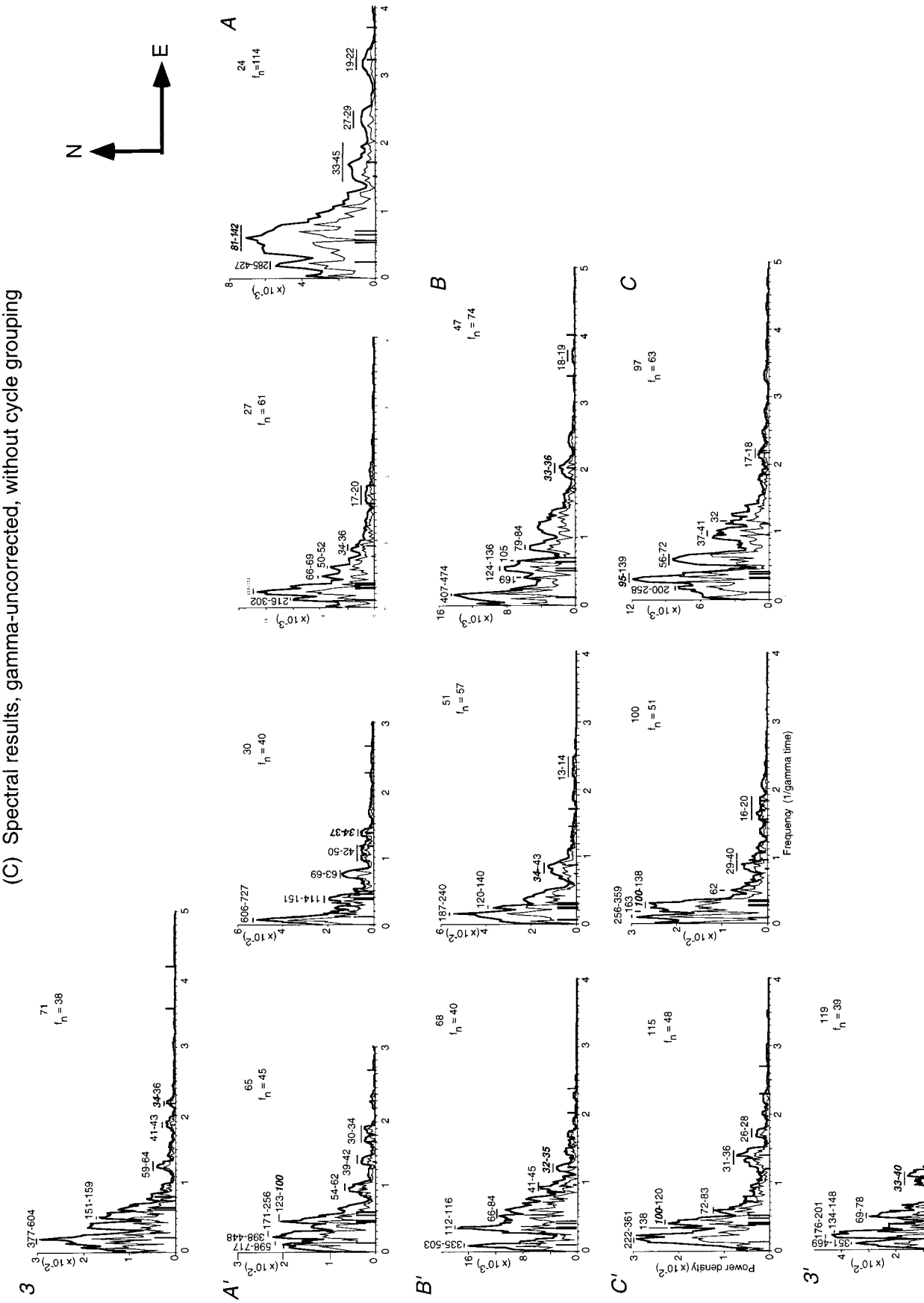

FIG. 10.—Continued.

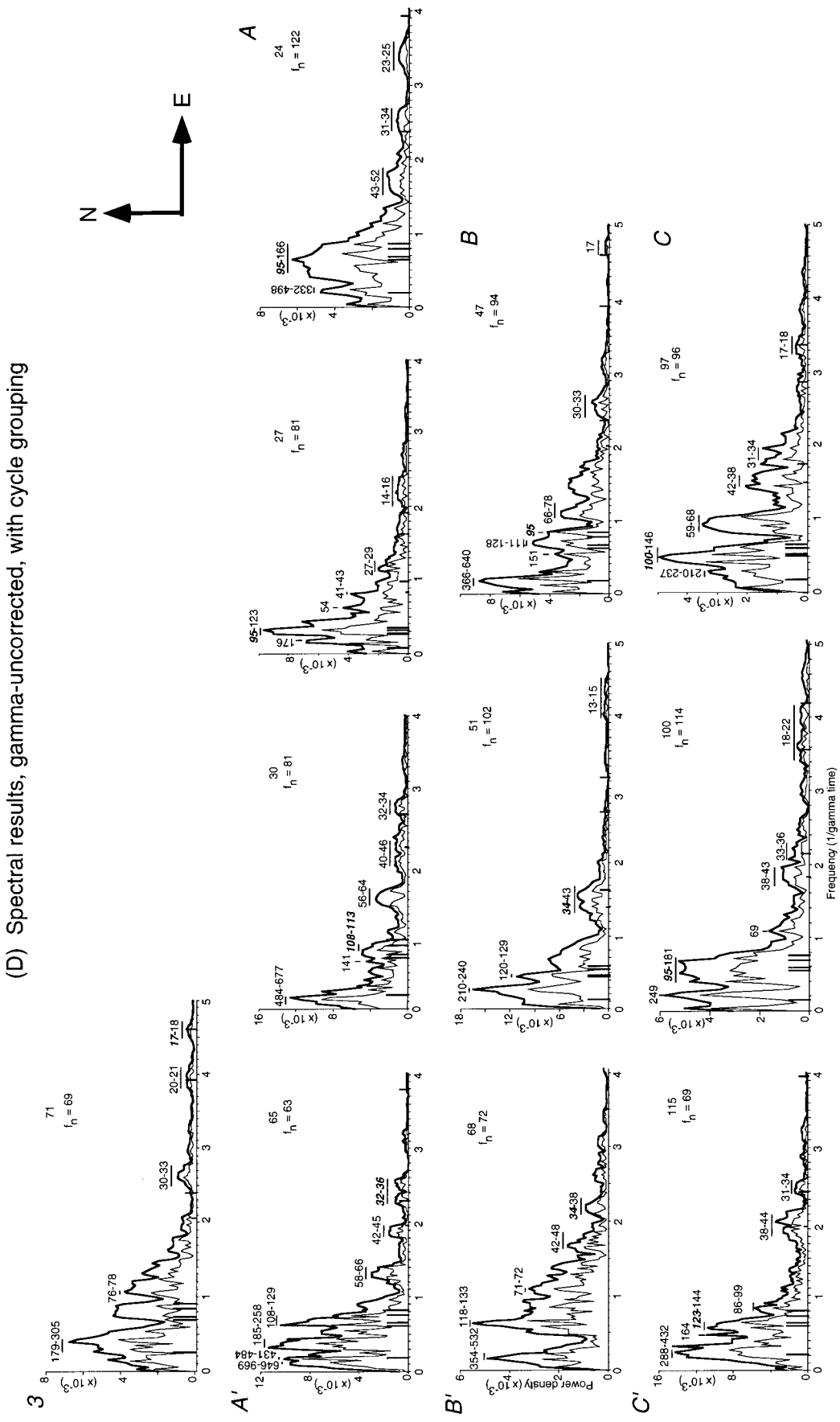

FIG. 10.—Continued.

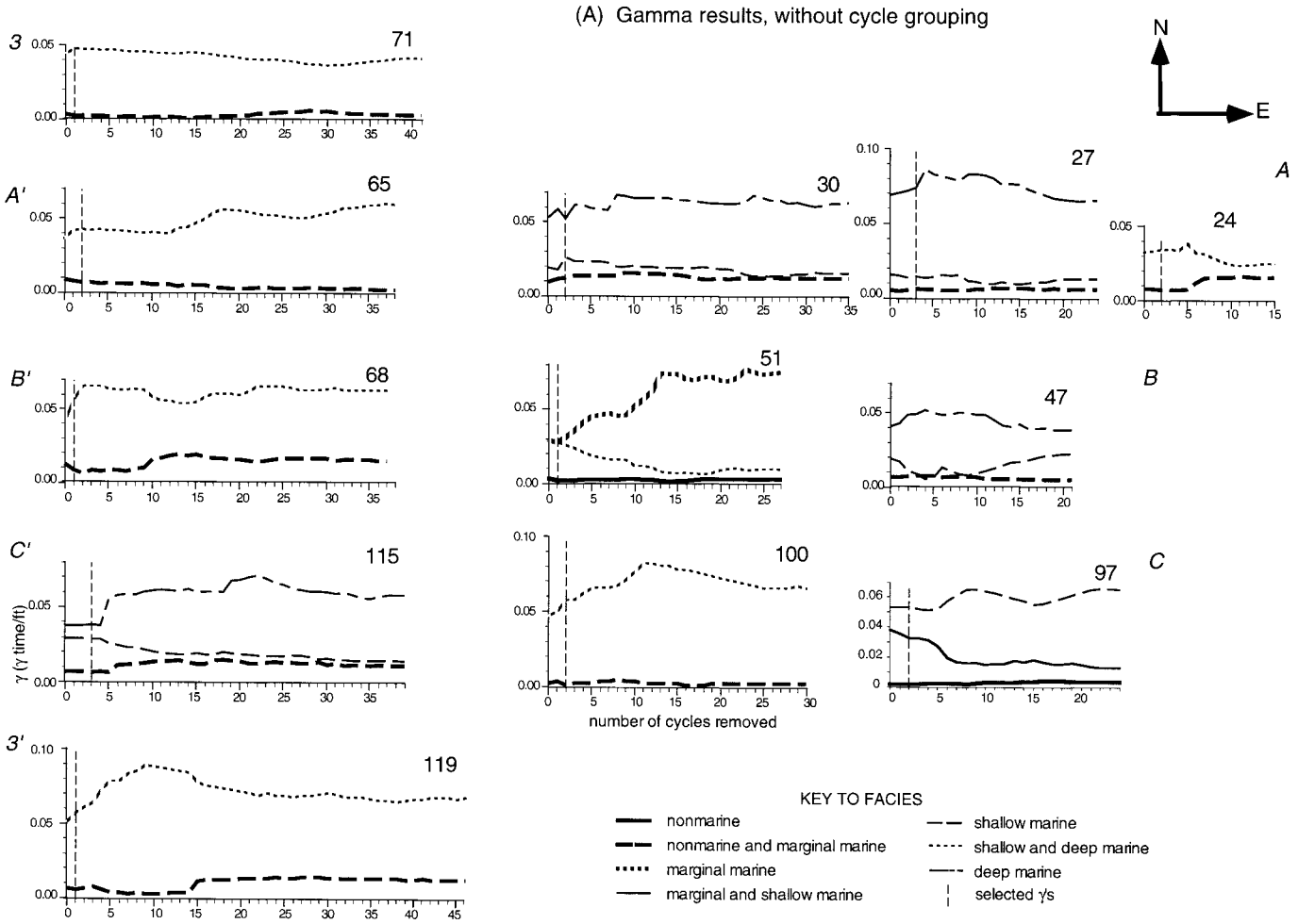

FIG. 11.—γ results of subsurface sections without and with cycle grouping [(A) and (B)]. See text for discussion.

primarily at precessional index periodicities. After 2.8 Ma, 41 ky variance increased markedly, coincident with the onset of bipolar glaciation. The dominance of 41 ky eolian variance after 1.6 Ma paralleled the development of enhanced 41 ky high-latitude glacial climate cycles. After 1 Ma eolian variability is dominated by 100 ky periodicity, coincident with marked increase of glacial climate extremes of a dominant 100 ky period (deMenocal 1995).

Glacio-eustasy and terrestrial climatic changes were the major controls on Cisco cyclicity (Yang 1996; Yang et al. 1998). The Cisco cycles were probably formed during glacial and terrestrial climate extremes on the gentle Eastern Shelf. Deglaciation-induced sea-level rises flooded the shelf, and large terrestrial climatic variations, such as monsoon intensity and tropical river outflow, caused large variations in sediment yield and supply (Yang 1996).

The dominance of 100 ky variance in the Cisco records probably reflects extreme glacial and terrestrial climatic conditions in Virgilian and Wolfcampian time. If the Cisco cycles were indeed deposited mainly during climate extremes, deposition would have been very limited, and erosion and nondeposition would have been extensive. As a result, a large amount of Cisco time is represented by unconformities, as suggested by the γ-estimated duration of the Cisco Group.

Cyclic sedimentation, however, was also controlled by other processes (Yang 1996; Yang et al. 1998; see also Brown 1969; Brown et al. 1990; Galloway 1971). The non-Milankovitch peaks may be the signatures of some of these processes. For example, the moderately consistent and well defined 25 ky peak may represent a non-Milankovitch allogenic process.

The 50–80 ky peak may have a Milankovitch orbital origin. In modeling a nonlinear climatic oscillator considering atmospheric, oceanic, cryospheric, crustal, and mantle interactions, LeTreut and Ghil (1983) predicted that the nonlinearly resonant response of the oscillator to Milankovitch astronomical forcings would lead to large changes in global temperature and ice volume, and the nonlinear character of the response also leads to linear combinations of the forcing frequencies. A combination tone, $(f_3\text{-}f_1+f_2)$, has a modern period of 66 ky, where f_1, f_2, and f_3 are the frequencies of short and long precessional index and short obliquity cycles. LeTreut and Ghil (1983) suspected that this peak, which is broadened by the rising chaotic background around it, accounts for the hump between 40 ky and 100 ky in the isotopic spectra of deep-sea cores V28–238 and RC11–209 (Imbrie and Imbrie 1980; Imbrie 1982).

The same combination tone has a period of 55 ky at 300 Ma and may correspond to the broadly defined but persistent 50–80 ky peak (Table 2). Combination tones, especially those between precessional index cycles, are commonly detected on spectra of ancient records (e.g., Bond et al. 1991, Kominz et al. 1991, Yang et al. 1995). They should be expected considering nonlinear interactions among various climatic and geologic processes.

This study suggests that the Cisco Group recorded dominant Milanko-

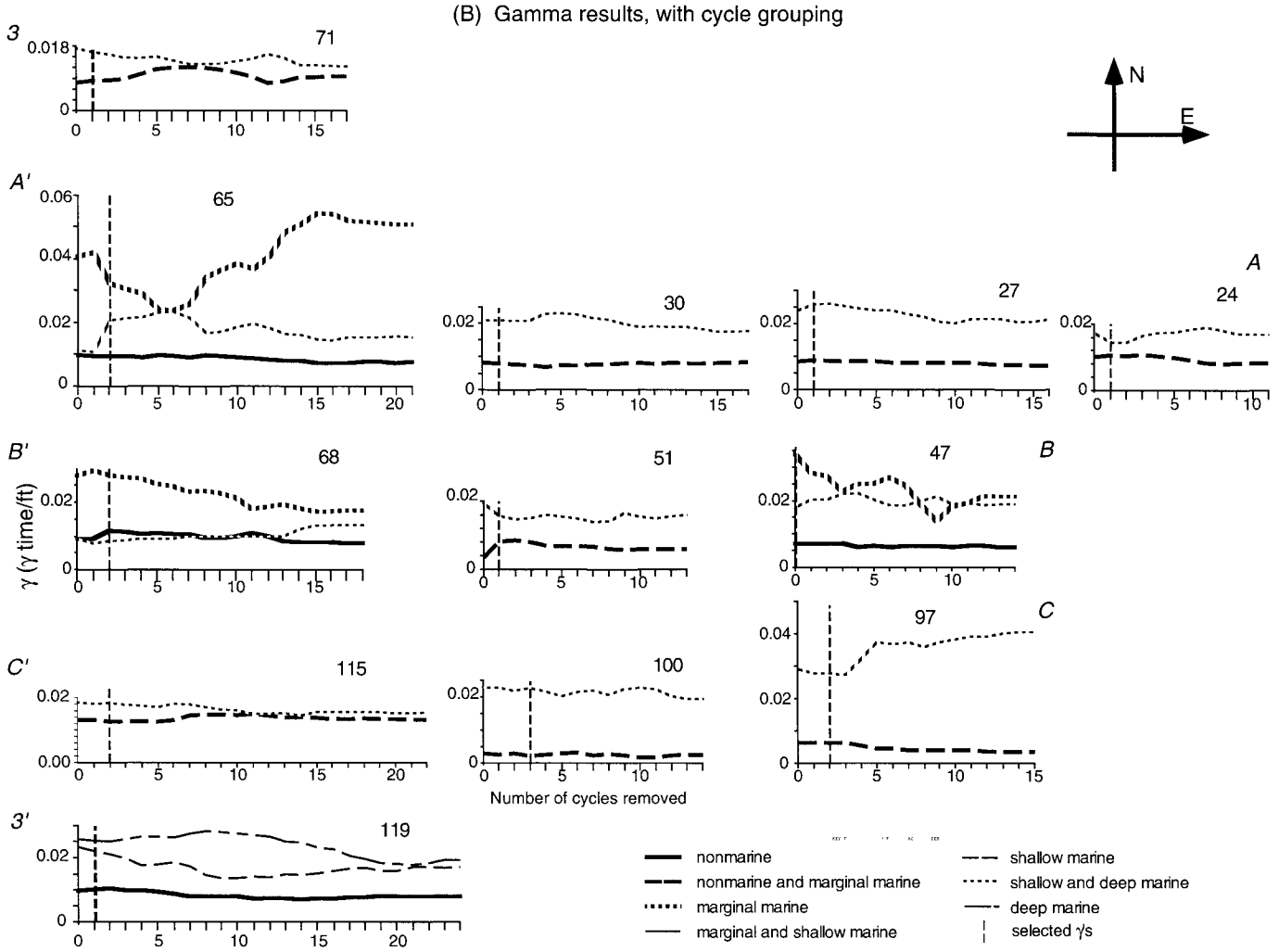

FIG. 11.—Continued.

vitch climatic cycles and other insignificant non-Milankovitch cycles. This supports the conclusions of geologic analysis: (1) an apparently autocyclic record does not imply the absence of allogenic processes, (2) a dominantly allogenic record may contain many autogenic imprints, and (3) no allogenic or autogenic process alone generated the Cisco cyclicity (Yang 1996; Yang et al. 1998).

SUMMARY

1. Positive and stable γ's of various facies of 30 sections provide a realistic thickness–time conversion to construct γ-corrected time series. γ-corrected spectra have higher resolution than uncorrected spectra and contain a maximum number of Milankovitch peaks.

2. Milankovitch peaks include a prominent and persistent short-eccentricity peak, persistent long-eccentricity and obliquity peaks, and nonpersistent precessional index peaks. A persistent 50–80 ky peak may be a combination tone of obliquity and precessional index cycles. Non-Milankovitch peaks include a fairly persistent 24–28 ky peak and other sporadic peaks.

3. Consistent age relations among the Cisco sections and reasonable sedimentation rates of various facies indicate the validity of gamma and spectral results.

4. Assuming that the γ-estimated Cisco duration is represented by rocks and that the chronostratigraphic duration is correct, only $\sim$ 6–25% of the Cisco time is recorded by rocks.

5. The Cisco cyclicity was controlled dominantly by Milankovitch climatic forcing and less significantly by other allogenic and autogenic processes. The mixed origin indicates that allogenic and autogenic processes combined to generate the Cisco cyclicity.

ACKNOWLEDGMENTS

This paper reports part of WY's dissertation research at The University of Texas at Austin. WY thanks Drs. J. Banner, G. Bond, W. Galloway, and R. Major for thoughtful discussions, and W. Dharmasamadhi, M. Li, and C. Kellam for field assistance. We thank D. Lehrmann, Associate Editors P. Myrow and B. Wilkinson, and an anonymous reviewer for critical reviews, G. Ashley and J. Southard for editorial comments, and the following individuals and institutions for access to data and equipment: P. Knox, R. Major, and Bureau of Economic Geology, The University of Texas at Austin; V. Jenkins and Mobil Oil Co.; M. Dusing and Coda Energy Co.; and Geomap Co. This work is supported by grants from Grant-in-Aid of the Geological Society of America, the DeFord Field Geology Fellowship of the Geology Foundation, The University of Texas at Austin, and Grant-in-Aid of the Gulf Coast Association of Geological Societies. Acknowledgment is made to the Donors of the Petroleum Research Fund, administrated by the American Chemical

Society under grants ACS-PRF 20852-AC8 and ACS-PRF 27102-AC8 to M. Kominz, which provided partial support for this research.

REFERENCES

Barrell, J., 1917, Rhythms and the measurements of geologic time: Geological Society of America, Bulletin, v. 28, p. 745–904.

Berger, A., 1988, Milankovitch theory and climate: Review of Geophysics, v. 26, p. 624–657.

Berger, A., Loutre, M.F., and Laskar, J., 1992, Stability of the astronomical frequencies over the Earth's history for paleoclimate studies: Science, v. 255, p. 560–566.

Boardman, D.R., II, and Malinky, J.M., 1985, Glacial-eustatic control of Virgilian cyclothems in north-central Texas, *in* McNulty, C.L., and McPherson, J.G., eds., Transactions, American Association of Petroleum Geologists, Southwest Section: Fort Worth Geological Society, p. 13–23.

Boardman, D.R., II, and Heckel, P.H., 1989, Glacial-eustatic sea-level curve for early Late Pennsylvanian sequence in north-central Texas and biostratigraphic correlation with curve for midcontinent North America: Geology, v. 17, p. 802–805.

Bond, G.C., Kominz, M.A., and Beavan, J., 1991, Evidence for orbital forcing of Middle Cambrian peritidal cycles: Wah Wah range, south-central Utah, *in* Franseen, E.K., Watney, W.L., Kendall, C.G.St.C., and Ross, W., eds., Sedimentary Modeling: Computer Simulations and Methods for Improved Parameter Definition: Kansas Geological Survey, Bulletin 233, p. 293–317.

Bond, G.C., Devlin, W.J., Kominz, M.A., Beavan, J., and McManus, J., 1993, Evidence of astronomical forcing of the Earth's climate in Cretaceous and Cambrian times: Tectonophysics, v. 222, p. 277–294.

Brown, L.F., Jr., 1969. Virgil–lower Wolfcamp repetitive depositional environments in north-central Texas, *in* Elam, J.G., and Chuber, S., eds., Cyclic Sedimentation in the Permian Basin: West Texas Geologic Society, p. 115–134.

Brown, L.F., Jr., Goodson, J.L., Harwood, P., 1972, Abilene Sheet: The University of Texas at Austin, Bureau of Economic geology, Geologic Atlas of Texas, scale 1:250,000.

Brown, L.F., Jr., Iriarte, R.F.S., and Johns, D.A., 1987, Regional stratigraphic cross sections, Upper Pennsylvanian and Lower Permian strata (Virgilian and Wolfcampian Series), north-central Texas: The University of Texas at Austin, Bureau of Economic Geology Cross Sections, 27 p., 27 plates.

Brown, L.F., Jr., Iriarte, R.F.S., and Johns, D.A., 1990, Regional depositional systems tracts, paleogeography, and sequence stratigraphy, Upper Pennsylvanian and Lower Permian strata, north-central Texas: The University of Texas at Austin, Bureau of Economic Geology, Reports of Investigations 197, 116 p., 27 plates.

Chappell, J., and Shackleton, N.J., 1986, Oxygen isotopes and sea level: Nature, v. 324, p.137–140.

Connolly, W.M., and Stanton, R.J., Jr., 1992, Interbasinal cyclostratigraphic correlation of Milankovitch band transgressive–regressive cycles: Correlation of Desmoinesian–Missourian strata between southeastern Arizona and the midcontinent of North America: Geology, v. 20, p. 999–1002.

Cronin, T.M., 1983, Rapid sea level and climate change: Evidence from continental and island margins: Quaternary Sciences Review, v. 1, p. 177–214.

Crowell, J.C., 1978, Gondwanan glaciation, cyclothems, continental positioning, and climate change: American Journal of Science, v. 278, p. 1345–1372.

deMenocal, P.B., 1995, Plio-Pleistocene African climate: Science, v. 270, p. 53–59.

Enos, P., 1991, Sedimentary parameters for computer modeling, *in* Franseen, E.K., Watney, W.L., Kendall, C.G.St.C., and Ross, W., eds., Sedimentary Modeling: Computer Simulations and Methods for Improved Parameter Definition: Kansas Geological Survey, Bulletin 233, p. 63–99.

Fischer, A.G., 1964, The Lofer cyclothems of the Alpine Triassic: Kansas Geological Survey, Bulletin 169, p. 107–149.

Galloway, W.E., 1971, Depositional systems and shelf–slope relationships in uppermost Pennsylvanian rocks of the Eastern Shelf, north-central Texas [unpublished Ph.D. thesis]: The University of Texas at Austin, Austin, Texas, 116 p.

Gilbert, G.K., 1895, Sedimentary measurement of geologic time: Journal of Geology, v. 3, p. 121–127.

Goldhammer, R.K., Dunn, P.A., and Hardie, L.A., 1990, Depositional cycles, composite sea level changes, cycle stacking patterns, and the hierarchy of stratigraphic forcing: examples from platform carbonates of the Alpine Triassic: Geological Society of America, Bulletin, v. 102, p. 535–562.

Goldhammer, R.K., Oswald, E.J., and Dunn, P.A., 1994, High-frequency, glacio-eustatic cyclicity in the Middle Pennsylvanian of the Paradox Basin: an evaluation of Milankovitch forcing, *in* de Boer, P.L., and Smith, D.G., eds., Orbital Forcing and Cyclic Sequences: International Association of Sedimentologists, Special Publications 19, p. 243–283.

Grotzinger, J.P., 1986, Cyclicity and paleoenvironmental dynamics, Rocknest platform, northwest Canada: Geological Society of America, Bulletin, v. 97, p. 1208–1231.

Hardie, L.A., Dunn, P.A., and Goldhammer, R.K., 1991, Field and modelling studies of Cambrian carbonate cycles—Discussion: Journal of Sedimentary Petrology, v. 61, p. 636–646.

Harland, W.D., Armstrong, R.L., Cox, A.V., Craig, L.E., Smith, A.G., and Smith, D.G., 1989, A Geologic Time Scale: Cambridge University Press, Cambridge Earth Science Series, 263 p.

Harrison, E.P., 1973, Depositional history of Cisco–Wolfcamp strata, Bend Arch, north-central Texas [unpublished Ph.D. thesis]: Texas Tech University, Lubbock, Texas, 189 p.

Hays, J.D., Imbrie, J., and Shackleton, N.J., 1976, Variations in the Earth's orbit: Pacemaker of the ice ages: Science, 194, p. 1121–1132.

Heckel, P.H., 1977, Origin of phosphatic black shale facies in Pennsylvanian cyclothems of Midcontinent North America: American Association of Petroleum Geologists, Bulletin, v. 61, p. 1045–1068.

Heckel, P.H., 1986, Sea-level for Pennsylvanian eustatic marine transgressive–regressive depositional cycles along midcontinent outcrop belt, North America: Geology, v. 14, p. 330–334.

Herbert, T.D., 1992, Paleomagnetic calibration of Milankovitch cyclicity in Lower Cretaceous sediments: Earth and Planetary Science Letters, v. 112, p. 15–28.

Hinnov, L.A., and Goldhammer, R.K., 1991, Spectral analysis of the Middle Triassic Latemar Limestone: Journal of Sedimentary Petrology, v. 61, p. 1173–1193.

Hinnov, L.A., and Park, J., 1998, Detection of astronomical cycles in the stratigraphic record by frequency modulation (FM) analysis: Journal of Sedimentary Research, v. B68, p. 524–539.

Imbrie, J., 1982, Astronomical theory of the Pleistocene ice ages: A brief historical review: Icarus, v. 50, p. 408–422

Imbrie, J., and Imbrie, K.P., 1979, Ice Ages; Solving the Mystery: Hillside, New Jersey, Enslow, 253 p.

Imbrie, J., and Imbrie, J.Z., 1980, Modeling the climatic response to orbital variations: Science, v. 207, p. 943–953.

Imbrie, J., Hays, J.D., Martinson, D., McIntyre, A., Mix, A., Morley, J., Pisias, N., Prell, W., and Shackleton, N.J., 1984, The orbital theory of Pleistocene climate: support from a revised chronology of the marine $\delta^{18}O$ record, *in* Berger, A.L., Imbrie, J., Hays, J., Kukla, G., and Saltzman, B., eds., Milankovitch and Climate, Part 1: Dordrecht, The Netherlands, Reidel, p. 269–305.

Klein, G.deV., 1990, Pennsylvanian time scales and cycle periods: Geology, v. 18, p. 455–457.

Kominz, M.A., 1996, Whither cyclostratigraphy? Testing the gamma method on Upper Pleistocene deep-sea sediments: North Atlantic Deep Sea Drilling Project Site 609: Paleoceanography, v. 11, p. 481–504.

Kominz, M.A., and Bond, G.C., 1990, A new method of testing periodicity in cyclic sediments—application to the Newark Supergroup: Earth and Planetary Science Letters, v. 98, p. 233–244.

Kominz, M.A., and Bond, G.C., 1992, Documenting the reliability and utility of the γ method as applied to cyclic sections using forward modeling: Earth and Planetary Science Letters, v. 113, p. 449–457.

Kominz, M.A. and Pisias, N.G., 1979, Pleistocene climate: Deterministic or stochastic? Science, v. 204, p. 171–173.

Kominz, M.A., Beavan, J., Bond, G.C., and McManus, J., 1991, Are cyclic sediments periodic? Gamma analysis and spectral analysis of Newark Supergroup lacustrine strata, *in* Franseen, E.K., Watney, W.L., Kendall, C.G.St.C., and Ross, W., eds., Sedimentary Modeling: Computer Simulations and Methods for Improved Parameter Definition: Kansas Geological Survey, Bulletin 233, p. 319–334.

Lee, W., 1938, Stratigraphy of the Cisco Group of the Brazos Basin: University of Texas, Publication 3801, p. 11–90.

LeTreut, H., and Ghil, M., 1983, Orbital forcing, climatic interactions, and glaciation cycles: Journal of Geophysical Research, v. 88, p. 5167–5190.

Mesolella, K.J., Matthews, R.K., Broecker, W.S., and Thurber, D.L., 1969, The astronomical theory of climatic change: Barbados data: Journal of Geology, v. 77, p. 250–274.

Olsen, P.E., 1986, A 40-million-year lake record of Early Mesozoic orbital climatic forcing: Science, v. 234, p. 842–848.

Park, J., and Herbert, T.D., 1987, Hunting for paleoclimatic periodicities in a geologic time series with an uncertain time scale: Journal of Geophysical Research, v. 92, p. 14,027–14,049.

Sadler, P.M., 1981, Sediment accumulation rate and the completeness of stratigraphic sections: Journal of Geology, v. 89, p. 569–584.

Sadler, P.M., 1994, The expected duration of upward-shallowing peritidal carbonate cycles and their terminal hiatuses: Geological Society of America, Bulletin, v. 106, p. 791–802.

Soreghan, G.S., 1994, The impact of glacioclimatic change on Pennsylvanian cyclostratigraphy, *in* Embry, A.F., Beauchamp, B., and Glass, D.J., eds., Pangea: Global Environments and Resources: Canadian Society of Petroleum Geologists, Memoir 17, p. 523–543.

Thomson, D.J., 1982, Spectrum estimation and harmonic analysis: Institute of Electrical and Electronics Engineers, Proceedings, v. 70, p. 1055–1096.

Veevers, J.J., and Powell, C.McA., 1987, Late Paleozoic glacial episodes in Gondwanaland reflected in transgressive–regressive depositional sequences in Euramerica: Geological Society of America, Bulletin, v. 98, p. 475–487.

Wanless, H.R., and Shepard, F.P., 1936, Sea level and climatic changes related to late Paleozoic cycles: Geological Society of America, Bulletin, v. 38, p. 1177–1206.

Wermund, E.G., and Jenkins, W.A., Jr., 1969, Late Pennsylvanian Series in north-central Texas, *in* Wermund, E.G., and Brown, L.F., Jr., eds., A Guidebook to the Late Pennsylvanian Shelf Sediments, North-Central Texas: Dallas Geological Society, American Association of Petroleum Geologists, Annual Meeting, p. 1–11.

Wilkinson, B.H., Opdyke, B.N., and Algeo, T.J., 1992, Time partitioning in cratonic carbonate rocks: Geology, v. 19, p. 1093–1096.

Wilson, J.L., 1967, Cyclic and reciprocal sedimentation in Virgilian strata of Southern New Mexico: Geological Society of America, Bulletin, v. 78, p. 805–818.

Witzke, B.J., 1990, Palaeoclimatic constraints for Palaeozoic palaeolatitudes of Laurentia and Euramerica, *in* McKerrow, W.S., and Scotese, C.R., eds., Paleozoic Palaeogeography and Biogeography: Geological Society of London, Memoir 12, p. 57–73.

Yancey, T.E., 1991, Controls on carbonate and siliciclastic sediment deposition on a mixed carbonate–siliciclastic shelf (Pennsylvanian Eastern Shelf of north Texas), *in* Franseen, E.K., Watney, W.L., Kendall, C.G.St.C., and Ross, W., eds., Sedimentary Modeling: Computer

Simulations and Methods for Improved Parameter Definition: Kansas Geological Survey, Bulletin 233, p. 263–272.

YANG, W., 1995, Depositional cyclicity of the Cisco Group (Virgilian and Wolfcampian), north-central Texas [unpublished Ph.D. thesis]: Austin, The University of Texas, 268 p.

YANG, W., 1996, Cycle symmetry and its causes, Cisco Group (Virgilian and Wolfcampian), Texas: Journal of Sedimentary Research, v. B66, p. 1102–1121.

YANG, W., HARMSEN, F., AND KOMINZ, M.A., 1995, Quantitative analysis of a peri-tidal carbonate sequence, the Middle and Upper Devonian Lost Burro Formation, Death Valley, California—A possible Milankovitch climatic record: Journal of Sedimentary Research, v. B65, p. 306–322.

YANG, W., KOMINZ, M.A., AND MAJOR, R.P., 1998, Distinguishing the roles of autogenic and allogenic processes in cyclic sedimentation, Cisco Group (Virgilian and Wolfcampian), north-central Texas: Geological Society of America, Bulletin, v. 110, p. 1333–1353.

Received 29 September 1997; accepted 9 April 1999.